

# Utilizing Martian Regolith for 3D Printing in Martian Conditions

Victoria Stulova

Supervisor: Reza Hedayati



Image by: National Geographic



# Utilizing Martian Regolith for 3D Printing in Martian Conditions

by

Victoria Stulova

to obtain the degree of Master of Science  
at the Delft University of Technology,  
to be defended publicly on Friday August 30, 2019 at 14:00.

Student number: 4363124  
Project duration: January 5, 2019 – August 30, 2019  
Thesis committee: Prof. Sybrand van der Zwaag TU Delft, chair  
Prof. Jos Sinke TU Delft  
Prof. Santiago Garcia TU Delft  
Reza Hedayati TU Delft, supervisor

An electronic version of this thesis is available at <http://repository.tudelft.nl/>.



# Preface

This report is the result of my research performed at TU Delft during the master thesis period. This research concerned the exploration of Martian regolith properties with respect to making a material 3D-printable in Martian conditions. Although there were many problems that had to be solved during the course of the project, it was overall a very exciting and intellectually enriching experience. Having to work on such a large project fully by myself was challenging at first, but with the support of those around me it went considerably smoother.

I would like to give the most gratitude to my supervisor Reza Hedayati, who kept the project pace going with useful tips and suggestions, and the leader of NOVAM Sybrand van der Zwaag, who helped to steer the project in a right direction to obtain the most useful results. Most of all, I would like to thank TU Delft for making these 5 years of my life interesting and highly enriching, culturally and intellectually.

*Victoria Stulova*  
*Delft, August 2019*



# Abstract

Limitations of manned missions include limited amount of payload that can be transported to the target body, and human vulnerability to harsh pressures, temperatures and space radiation. Hence, it is preferable that the potential landing location for humans has a constructed habitat that should preferably be made from in-situ materials before humans arrive. This means that the prospect of utilizing a readily available Martian material, such as regolith, in an easily programmable manufacturing method, such as 3D printing, is very lucrative. The goal of this project is to develop a mixture containing Martian regolith for the purposes of 3D-printing in unfavourable conditions.

Regolith has the properties that allow it to act as geopolymer in the presence of appropriate alkaline binder, and hypothetically a very low amount of such binder is needed. For the sake of this project, a simplified binder which consists of water and Sodium Silicate is used. Martian conditions are less favourable for the curing of such mixture because of low temperature and pressure on the surface of the planet. Manufacturing through 3D-printing, as compared to moulding, might also have an effect on the resultant mechanical properties. In order to evaluate mechanical properties of the mixture, sample moulding and 3D-printing was supposed to be conducted at various curing conditions, together with comparing the properties of resultant samples.

Because of the combination of low reaction speed at low temperature (2°C) and rapid water evaporation at low pressure (0.1 - 0.01 bar), curing of the samples at Martian conditions yielded unsatisfactory results. The reaction medium in the form of water was gone from the sample before the curing reaction could progress enough to form a proper geopolymer. Most of such samples were not robust enough to withstand the beginning of three-point bending test, yet alone to be used as a construction material. The samples cured at high temperatures (60°C) showed satisfactory results, with highest flexural load achieved up to 9 MPa when cured at 60°C temperature and 1 bar pressure. The samples that went through the 3D-printing procedure showed 20% worse results than moulded samples when it comes to ultimate flexural stress. Also, printing process itself did not go well because of the mixture curing rapidly under pressure and viscosity limitations.

Overall, the proposed mixture ended up being hardly suitable for the application because of high dependence on elevated temperature and pressure for curing. However, there is a good potential that modified binder composition with a hydroxide base incorporated might speed up the reaction and make the final product significantly stronger, especially with enhancing printing conditions using laser sintering, heat lamp or pressurised dome.





# Contents

|   |             |
|---|-------------|
| <b>Abstract</b>   | <b>v</b>    |
| <b>List of Figures</b>  | <b>ix</b>   |
| <b>List of Tables</b>   | <b>xi</b>   |
| <b>List of Symbols</b>  | <b>xiii</b> |
| <b>List of Acronyms</b>   | <b>xv</b>   |
| <b>1 Introduction</b>   | <b>1</b>    |
| 1.1 Background information. . . . .   | 1           |
| 1.2 Goals of the project. . . . .   | 2           |
| 1.3 Project roadmap . . . . .   | 2           |
| 1.4 Literature review . . . . .   | 3           |
| 1.4.1 Mission needs. . . . .  | 3           |
| 1.4.2 Difference between building manufacturing on Earth and Mars . . . . . | 4           |
| <b>2 Regolith Characterization</b>  | <b>7</b>    |
| 2.1 Density . . . . .   | 7           |
| 2.2 Particle Shape and Size . . . . .                                       | 8           |
| 2.3 Chemical Composition . . . . .  | 10          |
| <b>3 Binder Selection</b>   | <b>13</b>   |
| 3.1 Literature Propositions . . . . .                                       | 13          |
| 3.2 Selection Trade-off . . . . .   | 15          |
| 3.3 Pure Material Properties . . . . .                                      | 18          |
| 3.4 Chemical Properties . . . . .   | 19          |
| 3.5 Reaction Variations. . . . .  | 21          |
| 3.6 Curing Reaction in Practice . . . . .                                   | 23          |
| <b>4 Moulding Process</b>   | <b>27</b>   |
| 4.1 Mould preparation . . . . .   | 27          |
| 4.2 Sample Preparation . . . . .  | 28          |
| 4.3 Curing conditions of moulded samples . . . . .                          | 30          |
| <b>5 Additive Manufacturing Process</b>                                     | <b>33</b>   |
| 5.1 Printer Characteristic . . . . .  | 33          |
| 5.2 Printer settings . . . . .  | 35          |

---

|          |  |           |
|----------|--|-----------|
| 5.3      | Modifications to the printer and program . . . . . | 36        |
| 5.4      | Printing Observations . . . . .                    | 39        |
| 5.5      | Martian conditions. . . . .                        | 40        |
| 5.6      | Laboratory Environment Adaptation . . . . .        | 41        |
| 5.6.1    | Temperature Control . . . . .                      | 41        |
| 5.6.2    | Pressure Control . . . . .                         | 43        |
| <b>6</b> | <b>Results and Discussion</b>                      | <b>47</b> |
| 6.1      | Results. . . . .                                   | 47        |
| 6.1.1    | Mould removal . . . . .                            | 47        |
| 6.1.2    | Pore characteristics. . . . .                      | 50        |
| 6.1.3    | Density . . . . .                                  | 51        |
| 6.1.4    | Elastic Modulus. . . . .                           | 55        |
| 6.1.5    | Ultimate Flexural Stress . . . . .                 | 59        |
| 6.2      | Discussion of the Results . . . . .                | 63        |
| 6.3      | Application to Mars . . . . .                      | 64        |
| <b>7</b> | <b>Conclusion</b>                                  | <b>67</b> |
| <b>8</b> | <b>Recommendations</b>                             | <b>69</b> |
|          | <b>Bibliography</b>                                | <b>71</b> |

# List of Figures

|     |   |    |
|-----|---|----|
| 2.1 | SEM images of regolith powder with various particle sizes. . . . .  | 10 |
| 2.2 | EDX results from a MMS-2 regolith powder sample. . . . .  | 11 |
| 3.1 | Schematic representation of geopolymerization reaction [1]. . . . .   | 20 |
| 3.2 | The last step of forming a 3D polymeric network within geopolymer reaction (with Potassium instead of Sodium) [2] . . . . .   | 21 |
| 3.3 | Microscopic image of a mixture surface during saturation and gelation phases (x1000)  | 22 |
| 3.4 | DSC plots for curing the sample at 2°C, separated into two different time frames for clarity. (a) The first gelation step (time period 0 to 20 minutes). (b) The second gelation step (time period 0 to 250 minutes). . . . .   | 24 |
| 3.5 | Complete DSC plot for curing the sample at 23°C, including analysis of both cure steps. . . . .   | 25 |
| 3.6 | Complete DSC plot for curing the sample at 60°C, including analysis of both cure steps. . . . .   | 26 |
| 4.1 | The appearance of a mould in the drawn form and the printed form . . . . .  | 28 |
| 5.1 | Key components required for the 3D-printing process. a) Schematic representation of selected printer model with key components indicated [3]. b) Teaching pendant [4]. c) Digital fluid dispenser, responsible for pressure control [5] . . . . .   | 34 |
| 5.2 | Syringes used for 3D-printing with the provided printer. a) Manufacturer design, unsuitable because of narrow outlet. b) Redesigned syringe, with larges outlet possible in current situation. c) Rendering of the redesigned syringe . . . . .   | 37 |
| 5.3 | Printing pattern for the 3D-printed samples. Green lines are printed towards from the front, blue are printed away from the front. Top two levels are either deposited immediately or after 30 minutes, to test the mechanical property variance with printing delays. . . . .  | 38 |
| 5.4 | Partially assembled 3D-printing setup for simulating Martian conditions. Outside of the picture water temperature control unit is stationed. Some components which are mentioned further in the section are not included (silicon cover, coiled pipe, vacuum pump, drilled holes in the cylindrical chamber). . . . . | 42 |
| 5.5 | Components related to temperature control inside the printing chamber. a) a Peltier module [6]. b) Coiled pipe design. . . . .  | 43 |

|      |   |    |
|------|---|----|
| 5.6  | <b>Components composing enclosed space inside the printing chamber for pressure control. a) Transparent solid cylindrical chamber design. b) Silicon cover design. c) Schematic of the cover going on top of the cylindrical chamber. d) Cover mould design. . . . .</b>  | 44 |
| 6.1  | <b>Pictures of some of the moulded samples and corresponding observations. Number of tested samples indicates the amount of samples that were robust enough for starting three-point bending test without the sample being broken during the test initiation. . . . .</b>   | 49 |
| 6.2  | <b>Images of printed samples with initial binder concentration of 45%. a) 66% regolith, printed without delay . b) 67% regolith, printed without delay. c) 68% regolith, printed without delay. d) 66% regolith, printed with delay. e) 67% regolith, printed with delay. f) 68% regolith, printed with delay. . . . .</b>                                | 50 |
| 6.3  | <b>Comparison of resultant relative density values for moulded samples . . . . .</b>  | 52 |
| 6.4  | <b>Relative density results from the 3D-printed samples. Dashed lines indicate sample printed in one go, solid lines indicate sample with 30 min delay between deposition. . . . .</b>  | 53 |
| 6.5  | <b>Average relative density across all the samples for certain temperature and pressure conditions . . . . .</b>  | 53 |
| 6.6  | <b>Force-displacement curve as the result of testing one specimen in three-point bending test setup. A straight part of the curve is selected for elastic modulus calculations, with respective force and displacement values. Force is converted into stress, and displacement is converted into dimensionless value using sample thickness. . . . .</b> | 56 |
| 6.7  | <b>Three-point bending test setup with one of the moulded samples. . . . .</b>  | 56 |
| 6.8  | <b>Comparison of resultant elastic modulus values for moulded samples . . . . .</b>   | 57 |
| 6.9  | <b>Elastic modulus results from the 3D-printed samples. Dashed lines indicate sample printed in one go, solid lines indicate sample with delay. . . . .</b>   | 58 |
| 6.10 | <b>Average elastic modulus across all the samples for certain temperature and pressure conditions . . . . .</b>   | 58 |
| 6.11 | <b>Comparison of resultant ultimate flexural strength values for moulded samples . . . . .</b>  | 60 |
| 6.12 | <b>Ultimate flexural strength results from the 3D-printed samples. Dashed lines indicate sample printed in one go, solid lines indicate sample with delay. . . . .</b>  | 61 |
| 6.13 | <b>Average UFS across all the samples for certain temperature and pressure conditions . . . . .</b>   | 62 |

# List of Tables

|     |  |    |
|-----|--|----|
| 2.1 | <b>The results of density measuring experiment, together with a calculated average density.</b>  | 8  |
| 2.2 | <b>The results of dry sieving test on a bulk of regolith powder, including direct measurements and calculated percentages.</b>   | 9  |
| 2.3 | <b>MMS-2 regolith composition and actual Martian regolith composition as provided by the company [7].</b>  | 11 |
| 2.4 | <b>EDX results from a MMS-2 regolith powder sample adjusted for carbon and gold content.</b>   | 11 |
| 3.1 | <b>Binder trade-off results.</b>   | 17 |
| 4.1 | <b>The steps of making a moulded sample.</b>   | 29 |
| 4.2 | <b>Sample composition matrix for curing in room conditions.</b>  | 31 |
| 4.3 | <b>Sample composition matrix for curing other than room conditions.</b>  | 31 |
| 4.4 | <b>Temperature and pressure variation selected for the sample creation.</b>  | 32 |
| 6.1 | <b>Viability of tested samples with respect to cure conditions. Green cells indicate good conditions, yellow indicate conditions that produce somewhat useful material, red indicate poor cure conditions.</b> | 63 |



# List of Symbols

| <b>Symbol</b> | <b>Description</b>                      |
|---------------|---|
| $\rho_R$      | Density of the regolith powder          |
| $\sigma$      | Stress                                  |
| $\sigma_h$    | Stress at high point of the curve       |
| $\sigma_l$    | Stress at low point of the curve        |
| $d$           | Displacement                            |
| $d_h$         | Displacement at high point of the curve |
| $d_l$         | Displacement at low point of the curve  |
| $E$           | Elastic modulus                         |
| $e$           | Strain                                  |
| $e_h$         | Strain at high point of the curve       |
| $e_l$         | Strain at low point of the curve        |
| $F$           | Force                                   |
| $F_h$         | Force at high point of the curve        |
| $F_l$         | Force at low point of the curve         |
| $l$           | Sample length                           |
| $l_s$         | Bench span length                       |
| $P_c$         | Curing pressure                         |
| $T_c$         | Curing temperature                      |
| $t$           | Thickness                               |
| $m_{final}$   | Final mass                              |
| $m_{ini}$     | Initial mass                            |
| $V_{final}$   | Final volume                            |
| $V_{ini}$     | Initial volume                          |
| $w$           | Width                                   |





# List of Acronyms

|       |                                      |
|-------|--------------------------------------|
| DSC   | Differential Scanning Calorimetry    |
| EDX   | Energy-Dispersive X-ray spectroscopy |
| FDM   | Fused Deposition Modeling            |
| MMS-2 | Mojave Mars Simulant version 2       |
| PLA   | Polylactic acid $[C_3H_4O_2]_n$      |
| SEM   | Scanning Electron Microscopy         |
| UFS   | Ultimate Flexural Stress             |



# Introduction

## 1.1. Background information

Space exploration is an important societal and technological goal that potentially can provide humans with a considerable amount of knowledge and resources [8]. Since the Apollo 11 mission back in 1972, only highly specialized robots have been sent to other celestial bodies for in-situ exploration, as it is considerably safer and requires little supportive payload [9]. Robots, however, are quite limited in their functionality, as they are used for a particular number of scientific goals, programmed during the robot development [10].

Sending humans instead of robots would provide significantly more flexibility in research and valuable first-hand experience in the location to be explored. However, human lives are considerably more valuable than robots in case of a catastrophic failure, and require a lot of equipment in the form of food, water, shelter with all living necessities and space radiation protection at minimum [11]. Due to the latter in particular, the time a human can spend in space environment is very limited [12]. All these basic needs already force the mission to be considerably more expensive as compared to an unmanned one. Hence, to make the most out of manned mission, as much preparation as possible should be done before sending a human to other celestial body [13].

Because of a large sustaining equipment required for a manned mission together with necessary scientific equipment, expected amount of payload to be taken for a manned mission is very high. Therefore, as many in-situ resources as possible have to be utilized for both mission cost reduction and maintenance convenience [14]. Also, preparing the landing site for astronauts before they arrive can significantly increase the amount of useful research work that can be done in a set period of time, as space radiation limits the amount of time that humans can spend on other celestial bodies. Because of that, 3D-printing looks attractive as a manufacturing method for such purpose, as the desired design can be programmed in the printer and simply executed, provided that printing material is supplied [15–17]. If this printing material contains mostly in-situ gathered materials, the

amount of necessary payload can be significantly reduced [8].

This report concerns investigating the printing mixtures that can be utilized for Martian 3D-printing purposes, and selecting the most promising one. This mixture is then tested for overall viability at different manufacturing methods, namely moulding and printing, and the conclusion regarding the overall idea is made. As the starting point, Martian regolith is taken as primary material, as it is easy to collect and process from the surface of the planet, and the simulant of it is also purchasable online [18].

## **1.2. Goals of the project**

Main goal of the project is to find and develop a suitable binder/regolith mixture for Martian regolith 3D-printing application, and after a proper investigation make a conclusion about the viability of said mixture. In order to achieve this goal, various samples have to be constructed at different conditions, and the properties of these samples have to be compared.

Information that has to be gathered in order to achieve the goal includes looking at the properties of the selected binder/regolith mixture, cured at various conditions with two main processing methods: moulding and printing. The properties of interest for mixture include: curing reaction properties, visual pre-/ and post-cure properties, processing observations, density, and mechanical properties such as stress resistance and elastic modulus.

As the end result, the conclusion regarding the viability of this mixture has to be made, presented with potential improvements to both mixture and mixture selection process.

## **1.3. Project roadmap**

The beginning of the project was concerned with looking at the materials and items that can be utilized for the project goals. Chapter 2 covers the properties of obtained Martian regolith simulant, which include visual characteristics, density of the powder, particle size distribution, and elemental composition. Based on these properties and literature study, Chapter 3 explains the selection of the binder, including the trade-off between the options proposed by the literature, and further investigation of the selected binder properties. Curing reaction that involves regolith and selected binder is explained in the same chapter.

As the material selection is completed, Chapter 4 covers making of moulded samples from the selected materials, including design of the mould, selected curing compositions and conditions, and challenges regarding the moulding process. Printer and printed samples are investigated in Chapter 5, where printer description is provided, and the challenges related to printing the samples at room conditions and Martian conditions are described. The resultant samples were thor-

oroughly investigated and compared using visual, physical and mechanical testing, and the results are present in Chapter 6. Finally, conclusions and recommendations regarding the results are presented in Chapters 7 and 8 respectively.

## **1.4. Literature review**

Priorly to the beginning of work on this project, a literature review was conducted. In this section, some important considerations from this review are shown.

### **1.4.1. Mission needs**

On Earth, humans are adapted to the atmosphere conditions, are protected from space radiation by the atmosphere, and have an access to life-sustaining necessities such as oxygen, water, and food. In space, and in particular on Mars, atmosphere is almost negligible as compared to Earth, and life-sustaining resources are not readily available or even are absent. In order for humans to live for an extended amount of time on other celestial bodies, Earth-like conditions have to be maintained.

First of all, human body requires oxygen concentration, pressure, and temperature similar to the atmospheric conditions on Earth. This can be either provided by the space suits, which was done in short-term landings so far, or by the means of artificial atmosphere inside an enclosed location. For long-term missions, the second option is more desirable. This generates a structural requirement for the potential planetary habitat to withstand the inner pressure of artificial atmosphere on the habitat walls, minimize potential leakage of the artificial atmosphere and be able to withstand thermal loads, inflicted by the combination of high temperatures during the day, low during the night outside the habitat, and comfortable for humans inside the habitat.

Another pressing issue with human presence on other planets is space radiation, from which Martian atmosphere offers little to no protection. Even if it is possible to create a fully sustainable settlement on other than Earth planetary body, the duration of safe human stay in those settlements will be limited by space radiation. For Mars missions, which are considerably longer even with short period of stay due to long transfer time, the risks are considerably higher [12]. Walls of the habitat have to be sufficiently thick to absorb the incoming radiation and shield the humans inside [19]. Also, special attention has to be paid to the health of astronauts that are sent to the planetary missions, especially regarding genetics related to oncology and heart diseases. This can significantly decrease the mortality possibility due to radiation overdose [20].

When it comes to consumable resources, they can be transported from Earth. However in a long-term mission this is not an optimal solution due to the added mission costs associated with extra payload. It would be convenient to be able to produce and/or sustain the necessary items in the planetary outpost itself. Also, human wastes are better be recycled or at least destroyed to avoid stockpiling the wastes on the planets. These solutions are all associated with extra equipment

required for generating and recycling human consumables. Along with that, tools are required for processing those consumables, for example plates, glasses and cutlery when talking about food and water, or piping system when talking about hygiene. Using 3D printing however, it is convenient to be able to manufacture such tools fast and also be able to recycle them when damaged. The only items that have to be brought from Earth are printer parts and raw material (which takes less space than tools produced). Ease of recyclability compensates for possibly low mechanical properties of the tools.

#### 1.4.2. Difference between building manufacturing on Earth and Mars

**Transporting** any payload into space is very expensive comparing to transporting within the surface of the Earth. While there is a wide selection of materials that can be used for 3D printing on Earth, only a very limited amount can be reasonably transported into space. Taking enough material to build one or multiple habitats seems unrealistic, especially considering the fact that the walls have to be thick and strong to protect humans from dangerous environment. Hence, it is necessary to use in-situ resources when constructing the habitat, and potentially utilize in-situ resources for synthesis of usable binders. By exploring the underground of the planets, it could be possible to dig and construct an underground shelter, which offers high protection from meteoroid strikes and radiation due to the potentially high wall/ceiling thickness. However, for this to become possible more exploration is required. If the raw resources are not usable, perhaps the possibility of synthesizing a printing material would be open once more information about availability of those resources is known. This would require extra energy and possibly complex equipment, but the result might make the Martian colony independent from Earth.

Due to near-absence of atmosphere on Mars, small space objects like **meteors and asteroids** cannot be incinerated by the impact with atmosphere, like it happens around Earth. Instead, these small celestial bodies collide with the surface of Mars. On Mars, 30800 kg of meteoroid mass strikes the surface per day [21]. Earth receives considerably less meteoroid mass (between 2900 and 7300 kg per year, excluding dust particles), and it is slowed down by the atmosphere considerably [22]. The danger of meteoroid impact persists not only for potential humans and habitats on Mars, but also for the 3D printing equipment and unfinished habitat. Printing equipment itself can contain vulnerable components which might get damaged by smaller strikes. Initial stages of printing, which are expected to be most vulnerable due to unfinished structures and exposed printing equipment, are expected to be done without supervising humans, eliminating the possibility of easy repair. Material for building the habitat should also have enough impact resistance to withstand small strikes. It is not possible to completely prevent the impacts of meteoroids with the Moon or Mars, hence there is always a chance that a space rock might collide with the working location.

Unlike on Earth, where the presence of atmosphere and water stabilizes the temperature in individual regions, Mars has large **temperature variations** during the day/night cycles. Martian surface also experiences a swing from  $-153^{\circ}$  to  $+20^{\circ}$  near the equator. Near the poles, just like on

---

Earth, day/night cycles are considerably longer, hence the temperature swings are smaller. Temperature affects 3D printing and material cure to a very large extent, and therefore printing machines, processes, materials and habitat location have to be established together, as they affect each other closely. Near-vacuum conditions due to thin atmosphere make the problem worse, especially if the binder which is used to solidify Martian regolith is a liquid. On Earth, evaporation behaviour of liquids is governed by the presence of water vapour in the atmosphere. However, atmosphere is nearly absent on Mars, and hence no water vapour is present. This would result in deposited liquid rapidly evaporating into the ambient and, immediately afterwards, freezing due to low temperatures.





# 2

## Regolith Characterization

The main objective of this research is adapting Martian regolith for 3D-printing potential habitats on the Martian surface. For optimal analysis of regolith applications, it is necessary to learn about the properties of regolith. Knowing the properties can broaden the search for an optimal binder and contribute to the actual binder trade-off.

Regolith characterization starts with obtaining the powder density results, explained in Section 2.1, which can help in evaluating the density of resultant samples further in the report. Section 2.2 describes the sizes and shapes of particle in regolith simulant. Section 2.3 presents the results of EDX analysis that concerns chemical composition of the regolith powder.

### **2.1. Density**

In order to design a habitat from a given material, it is necessary to know the density of said material. Density, together with necessary wall thickness, allows to estimate the resultant structural weight, which in turn contributes to finding out weight-related stresses. This is especially important for space structures, as the wall thickness is expected to be quite high to provide necessary space radiation protection. Density of the raw powder can be used as a reference for comparing the densities of moulded and printed samples, as it makes the numbers easier to process. Besides, raw powder density might be important in design of the supporting equipment such as regolith collecting machines and paste mixing machines, allowing to determine maximum weight/volume ratio of regolith collected in one go. Besides, lower density of regolith can also mean lower mixture and therefore cured material weight, which in turn relaxes the mechanical property requirements from the material. Considering that regolith is present on Mars in large quantities, this is a positive point.

A bulk of regolith is essentially sand, which consists of small grains of various oxides. The size and shape of those particles is described further in Section 2.2. Because of sand-like structure, there is plenty of empty space between the grains. Measuring volume of the powder as it is can produce

varying results depending upon the packing of the grains, whether they were compressed or not. Besides, regolith is always used together with liquid binder in the scope of this report. Therefore, to produce more consistent results, the density of regolith is measured inside a measurement cylinder filled with water. Initial water level/volume is recorded inside the measuring cylinder, which is placed upon the scales. A portion of regolith is then added to this water, and weight difference together with volume difference is recorded. From these measurements, density can be determined as:

$$\rho_R = \frac{m_{final} - m_{ini}}{V_{final} - V_{ini}} \quad (2.1)$$

The resultant measurements then were processed into average density, which was taken as a reference density for the purpose of this report. The measurements can be seen in Table 2.1. As it can be seen from the results, the calculated average density of wet regolith is  $1873 \text{ kg/m}^3$ , with a standard deviation of  $128.4 \text{ kg/m}^3$ . This is comparable to the density of wet sand, which equals to  $1922 \text{ kg/m}^3$ . This value is going to be used as the reference density for comparing the sample densities and calculating relative densities, which in turn will contribute to analysis of mechanical properties. As an additional observation, it was noted that regolith particles were uniformly distributing themselves within the liquid without much additional mixing required. This was a positive observation with respect to selecting a regolith/binder combination for printing purposes, as the solution seemed to form easily without much additional interference.

Table 2.1: The results of density measuring experiment, together with a calculated average density.

| Test #         | Initial volume [ml] | Final volume [ml] | Volume difference [ml] | Mass difference [mg] | Density [ $\text{kg/m}^3$ ] |
|----------------|---------------------|-------------------|------------------------|----------------------|-----------------------------|
| 1              | 18.2                | 19.3              | 1.1                    | 2.04                 | 1854.5                      |
| 2              | 21.2                | 23.6              | 2.4                    | 4.21                 | 1754.2                      |
| 3              | 24.1                | 25.2              | 1.1                    | 2.26                 | 2054.5                      |
| 4              | 25.2                | 26.3              | 1.1                    | 2.01                 | 1827.3                      |
| <b>Average</b> |                     |                   |                        |                      | 1872.6                      |

## 2.2. Particle Shape and Size

While density measurement contributed to understanding the properties of bulk regolith, it is also useful to look at individual particles of the powder. Particle size and shape can affect the reaction parameters such as dissolution within the binder, as well as restrictions in temperature and pressure. Small and smooth particles are expected to spread within the binder mass at a higher rate with lower effort, and hence decrease the minimum amount of binder that is required for paste forming. At the same time, in the conditions where the pressure is low and ambience contains no water vapour, the binder solution evaporation happens at a considerably higher rate. Low temperatures cause preliminary freezing of the binder and halt curing reaction. Large and rough particles might

help trap the binder within the paste and prevent it from escaping into ambience and subsequently freezing, thus expanding the temperature and pressure reaction window. Considering that conditions on Mars involve low temperatures and pressures, these considerations are important to take into account.

Regolith particle dimensions were analysed using the dry sieve test. A bulk of regolith was sieved through 125  $\mu\text{m}$  and 63  $\mu\text{m}$  sieves, and resultant weight percentages were measured. As the amount of sieved regolith was relatively large (83 g as recorded in the end), there was no need to perform multiple sieve tests, as the result is seen to be representative enough. The weight fractions of dry sieve test on the regolith is presented in Table 2.2.

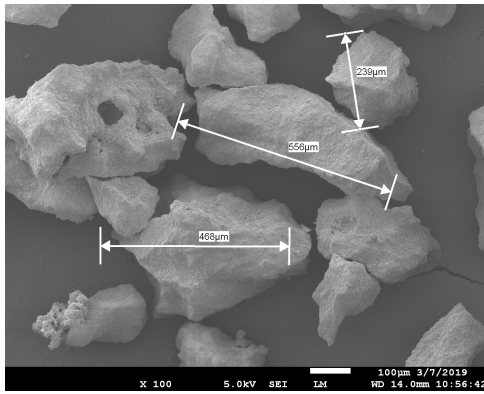
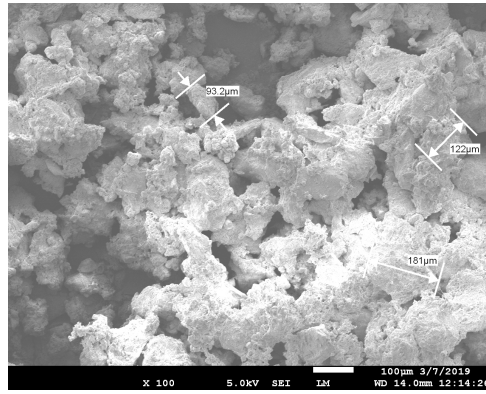
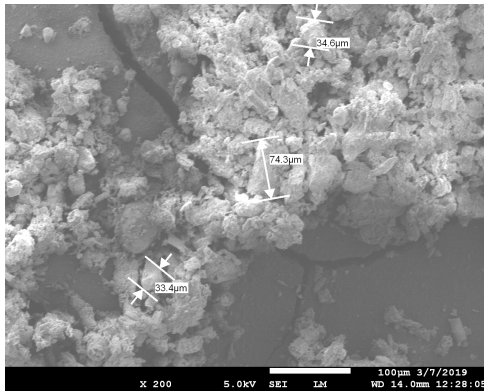
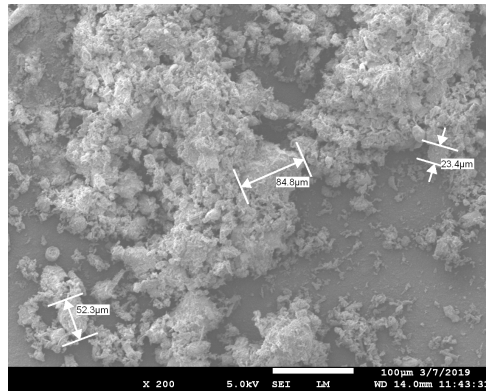
Table 2.2: The results of dry sieving test on a bulk of regolith powder, including direct measurements and calculated percentages.

| Sieve size [ $\mu\text{m}$ ] | >125  | 63-125 | <63   | Total |
|------------------------------|-------|--------|-------|-------|
| Mass [g]                     | 17.38 | 38.86  | 26.52 | 82.76 |
| Mass [%]                     | 21    | 47     | 32    | 100   |

Overall, it can be seen that majority of particles are smaller than 125  $\mu\text{m}$ . However, dry sieving does not give any indication regarding the particle shapes. For that, SEM (Scanning Electron Microscopy) imaging was used. Together with SEM, EDX (Energy-Dispersive X-ray spectroscopy) analysis was also performed, but the results of it will be addressed later in this report.

SEM imaging was preferred over optical microscopy in this case as it is easier to find images of high quality due to smaller influence of depth of view. The possibility of EDX analysis performed at the same time also contributed to making this choice. Sieved powder samples were placed upon a layer of carbon paint in order to both make the imaging possible and fix the powder upon the base cylinder, so that contamination of the chamber could be avoided. Carbon paint makes the sample conductive and protects it from a harsh vacuum environment. Also, the use of carbon paint reduces the possibility of imaging artifacts due to sample overcharge and prevents contamination of the chamber. Because of powdery nature of the sample, contamination risk is high and has to be reduced as much as possible to avoid issues with the apparatus. Excess powder particles that did not attach to the paint were shaken off the sample. Then, samples were coated with carbon on top to improve image quality. The resultant images are shown in Figures 2.1a to 2.1d.

From the SEM images, it can be seen that in general particles have irregular shapes, ranging from nearly spherical to highly elongated. Larger the particles are, higher the chance that the shape deviates from spherical. As it can be seen on the image, particles of medium and small size are closely packed, while large particles are mostly located apart from each other. Between the medium and small particles, porosity can be observed, meaning that liquid can potentially get between the particles easily without much mixing required, and initiate the curing reaction.

(a) Large ( $> 0.125\text{mm}$ ) sieved particles (x100).(b) Medium ( $0.063\text{mm} < x < 0.125\text{mm}$ ) sieved particles (x100).(c) Small ( $< 0.063\text{mm}$ ) sieved particles (x200).

(d) Unsieved particles (x200).

Figure 2.1: SEM images of regolith powder with various particle sizes.

As expected, the image with unsieved powder sample contains only smaller particles, considering how similar it is to the small powder image. This can be explained by the fact that small powder adhered to the carbon paint faster than the rest of the powder, and larger particles were not attached well enough because of limited vacant space, and fell off during excess shaking process. It means that regolith powder is not likely to be densely packed, otherwise the large particles like on Figure 2.1a would have been observed on the unsieved sample.

### 2.3. Chemical Composition

The purchased regolith had approximate composition indicated on the package. The regolith composition as indicated on the packaging is shown in Table 2.3. Approximate composition can be derived from this information, however to look at the whole picture a more exact measurement made by EDX is required. As it can be seen from the composition, a large amount of silicate oxide and aluminum oxide is present in regolith, which indicate suitability for geopolymer base, meaning that geopolymer binder can be investigated among other options.

Table 2.3: MMS-2 regolith composition and actual Martian regolith composition as provided by the company [7].

| Compound                        | MMS-2<br>(simulant name) | Mars |
|---------------------------------|--------------------------|------|
| Silicates ( $SiO_2$ )           | 44%                      | 44%  |
| Iron Oxide<br>( $Fe_2O_3$ )     | 18%                      | 18%  |
| Aluminum Oxide<br>( $Al_2O_3$ ) | 13%                      | 9%   |
| Calcium Oxide<br>( $CaO$ )      | 8%                       | 6%   |
| Magnesium<br>Oxide ( $MgO$ )    | 7%                       | 7%   |
| Sulfate ( $SO_2$ )              | 6%                       | 6%   |
| Trace                           | 4%                       | 11%  |

EDX measurements were performed during SEM measurements, and the results as given by the apparatus are presented in Figure 2.2. For this, magnification over the sample with unsieved powder was decreased such that a larger amount of powder could be taken into account. The resultant analysis produced a high percentage of carbon and some percentage of gold, which was the result of carbon paint and gold coating, which were necessary for SEM measurements. Carbon and gold are not important components of the regolith powder for planning a printing paste, and also they are not listed as primary elements in the composition indicated by manufacturer. Therefore, EDX result adjustment was performed and is shown in Table 2.4, which excluded carbon and gold from calculations. Copper and zinc were also excluded from calculations, as presence of those are a result of carbon paint being too thin or cracked in some locations, hence the composition of sample holder was recorded instead.

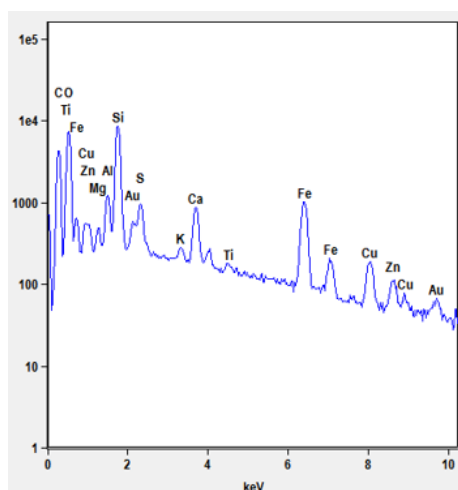


Figure 2.2: EDX results from a MMS-2 regolith powder sample.

Table 2.4: EDX results from a MMS-2 regolith powder sample adjusted for carbon and gold content.

| Element | EDX result [%] | Adjusted EDS result (no paint) [%] | Element composition calculated from manufacturers data [%] |
|---------|----------------|------------------------------------|--|
| O       | 29.97          | 62.05                              | 43.07  |
| Si      | 7.64           | 15.82                              | 20.53  |
| Fe      | 6.86           | 14.20                              | 12.6   |
| Ca      | 1.54           | 3.19                               | 5.71   |
| S       | 0.95           | 1.97                               | 3  |
| Al      | 0.87           | 1.80                               | 6.88   |
| Mg      | 0.22           | 0.46                               | 4.2  |
| K       | 0.13           | 0.27                               | -  |
| Ti      | 0.12           | 0.25                               | -  |
| C       | 46.89          | -                                  | -  |
| Au      | 1.01           | -                                  | -  |

As expected, oxygen is indicated as a most present element, which is clear from the fact that regolith mostly consists of various oxides. The amount of magnesium seems to be lower than what is provided on the packaging, but the percentage of other elements follow the pattern that is presented by manufacturer. Among the trace elements, potassium and titanium are detected by EDX, and it is possible that copper, zinc, carbon and gold are among the trace elements as well. Overall, the EDX analysis confirms the composition as indicated by manufacturer, considering the measurement was done over a small sample of powder without large particles present.

# 3

## Binder Selection

Knowing the properties of the regolith powder, potential binders can be looked at. Besides reacting with or incorporating regolith, other trade-off criteria also exist and can affect the decision. After selecting the binder, chemical properties of it have to be known in order to optimize the sample production process.

Section 3.1 covers the literature propositions that were considered for the role of regolith binder in this project. Section 3.2 explains the trade-off performed as a part of binder selection. As the binder material is selected and purchased, Section 3.3 provides a short description of the material regarding visual properties and storage conditions, and looks at the properties of binder solution, which is going to be mixed with regolith to form a printing paste. The chemical properties of the paste made with binder solution and regolith are shown in Section 3.4. Variations of the chemical properties of such paste are discussed in Section 3.5. Finally, explained chemical reaction is looked at in practice in Section 3.6.

### **3.1. Literature Propositions**

Manned Mars exploration has been a research subject for some time. Among other aspects, potential building materials have been looked at by various articles. Upon the review of these articles, several main options were chosen for the binder trade-off process, as those were looked at the most and seemed most promising. These options are: molten sulphur [23], Portland cement [24], geopolymer cement [25], and polymers such as polyimides and epoxies [26].

Molten sulphur upon mixing with a solid additive, in this case regolith powder, can form a strong concrete material that can be processed into a large structure, for example a building [23]. The mechanical properties of sulphur concrete are quite high, and together with reinforcement it can potentially make a strong structure. However, the processing limitations of sulphur concrete are strict and require high temperatures (up to 150°C). The procedure of extracting sulphur requires tem-

peratures even higher than that (around  $1100^{\circ}\text{C}$ ). Also, the curing behaviour of this mixture in the conditions of low temperature and pressure is unknown. Looking at mechanical properties, a major disadvantage lies in poor performance when subjected to thermal cycles, which are expected on other planets. From practical point of view, working with sulphur at high temperatures is dangerous in laboratory environment, and the printer obtained for the purpose of the project is unsuitable for working in high temperatures.

Portland cement is a reliable material which is widely used on Earth for various constructions. It was proposed to be also used on other celestial bodies, in particularly Moon, because of explored and strong mechanical properties and a large amount of knowledge available from the experience [24]. Large disadvantages of this mixture include, however, a relatively low calcium content of Martian regolith, and high processing temperatures (up to  $1450^{\circ}\text{C}$ ) required for calcination and sintering of the cement mixture. The cure in low pressure and temperature conditions (for example  $T_c = 2^{\circ}\text{C}$  and  $P_c = 0.01$  bar) for cement also is considerably slower (around 40 days) as compared to that in room temperature conditions (around 7 days) [27]. Also, such cement materials perform poorly when being subjected to thermal cycles.

Geopolymer concrete is based upon the reaction between precursor rich with silicon and aluminum and an alkaline solution. Typically, this solution consists of sodium silicate and a strong base like sodium hydroxide [28]. Unlike Portland cement, the processing conditions for geopolymer cement are simple and do not require high temperatures [1]. While higher processing temperature and pressure are preferable for cure purposes, cure can also occur in other conditions, only restricted by solution freezing temperature [29]. Literature mentions that the amount of binder required is quite low, and can potentially be as low as 98% regolith to binder ratio, which looks promising when it comes to transportation limitations. The expected disadvantage of this mixture is its poor performance at low temperature and pressure despite the reaction occurring [25].

Finally, the option of using polymers such as epoxies and polyimides was mentioned by several literature sources [26, 30]. Instead of being part of an activator, regolith would serve simply as a filler in such system, reducing the amount of polymer solution required for a bulk of material. Because of this, the amount of such polymer required for a bulk of material is quite high as compared to aforementioned concrete mixtures. For example, LaRC-SI based mixture would require at least 20% of solution, with 40% being a more optimal ratio. The usage of such polymers for building material on Moon or Mars is not quite explored by the literature, and is potentially a good solution for building in extreme ambient conditions. However, such solutions are usually expensive and are required in large quantities, making the transportation aspect questionable.



### 3.2. Selection Trade-off

The selection of binder material was performed through a trade-off process. Several criteria that were deemed important for both the project and practical application were chosen. Each criterion has a weight of 0 to 3, and the weightings are explained together with each criterion. It should be noted that the trade-off weighting is performed based upon literature and not experimental results, hence it might not be precise with respect to real situation. The criteria are:

- **Processing conditions** concern the complexity of the preparation and curing cycle when it comes to that particular regolith/binder mixture. This includes the total number of steps to prepare and cure the mixture, required temperature and pressure conditions. This affects not only the amount of time and resources needed for laboratory testing conditions, but also the processing complexity on Mars, increasing the amount of risk associated with the mission. A very important criterion for this research in particular, this criterion gets a weight of 3. 0 is going to mark processing that is nearly impossible in laboratory conditions, 1 means hardly possible without significant money and time investment, 2 means moderate amount of effort put into processing, and 3 means a simple cycle that can be done quickly and without much money investment.
- **3D-printing possibility** signifies the ease of performing 3D-printing with a mixture in question in laboratory conditions. The printer for this project was chosen beforehand and is described in Chapter 5, hence this choice introduces restriction in mixture viscosity and processing temperature. Another vital criterion for this project, assigned weight for it is 3. 0 indicates a mixture of too high viscosity or processing temperature that is not supported by current printer, 1 indicates hardly printable mixture that requires significant adjustments and has to sacrifice mechanical properties in order to be printed, 2 indicates a mixture that can be printed with some adjustments and within a certain property range, and 3 marks the mixture that can be easily printed without adjustments required.
- **State of research** is a criterion that affects the reliability of the trade-off and the risk of failure because of little information known. This criterion is less important than the previous ones, as even a failed result can be explained and recorded, thus providing more information about the mixture for a future research, not only in the area of space 3D-printing but for other applications. However, considering general time restriction on such projects, it is better to go for a more reliable option, hence this criterion is present with a weight of 2. 0 indicates a binder suggestion that is merely a concept and has not been explored yet, 1 indicates a binder that has been explored in non-extreme conditions and can hypothetically be applied in space, 2 stands for binder that was tested for similar applications and has some results when applicable to space related research, and 3 stands for binder that is known for good performance in harsh conditions.
- **Mechanical properties in extreme conditions**, or robustness as called later, is seemingly an important criterion that should eliminate some binder propositions due to poor performance

in Martian conditions. However it is always possible to introduce reinforcements into the structure that would help the resultant material to hold the loads [31]. Regardless, not having to rely upon reinforcements is a major positive point for such application, as it means that less payload has to be brought for building purposes. Also, low performance in cycling temperature conditions restricts the potential landing site locations. As poor robustness can partially be bypassed by adding reinforcements and adjusting structure, the weight of this criterion is 2. 0 indicates very poor performance in the conditions of low pressure and temperature swings, 1 indicates acceptable, but not reliable enough performance, 2 indicates such performance that theoretically should be minimally affected by the Martian conditions, and 3 indicates performance optimized for low pressure and temperature conditions.

- **Transportation viability** is only relevant to a real space mission situation, where each kilogram of payload significantly increases the total mission price, and hence should be minimized. This criterion does not affect the laboratory results at all, hence the weighting for this criteria is 1, which is low as compared to processing conditions and 3D-printing possibility. 0 indicates the mixture that would require an unrealistic amount of binder material and supportive equipment to be transported, while 3 indicates a material that is present on Mars and does not require large equipment besides 3D-printing one. 1 and 2 indicate transportation extents in between 0 and 3.
- **Price** is another minor factor when it comes to this trade-off, with a weight of 1. On a large scale of practical application, conducting a space mission is already a very expensive task. In that scenario, it might be more worth to invest a higher amount of money in a more expensive material that would perform more reliably than a cheaper alternative. On a smaller scale, in particular in laboratory conditions, a relatively small amount of material is needed for the experiments, as the sample sizes planned for experimental measurements are quite small. Nevertheless, price is still something that has to be accounted for. 0 indicates a relatively expensive material, 1 stands for a material with high, but acceptable price, 2 represents a cheap material, while 3 indicates a material that can be obtained on the surface of Mars, hence free one.

Based upon listed criteria, the trade-off was performed. The summary in a form of numerical scores is indicated in Table 3.1.

Sulphur has the advantage of being present not very deep from the surface of Mars, hence requiring only processing equipment, although large amount of the equipment because of extracting complexity [32]. Therefore, it earns 2 and 3 points in transportation and price respectively. It is covered by multiple papers as an option for Martian habitats, and decent amount of measurements and evaluations has already been done, earning 2 points in state of research. It is known that sulphur concrete has difficulties withstanding temperature swings and requires some reinforcements for optimal performance, giving it 1 in robustness. However, processing gets a 0, as working with sulphur is dangerous and requires very high temperatures. This is not only an issue in lab conditions,

Table 3.1: **Binder trade-off results.**

| Material [Weight]     | Sulphur   | Portland Cement | Geopolymer Concrete | Polymers  |
|-----------------------|-----------|-----------------|---------------------|-----------|
| Processing [3]        | 0         | 1               | 3                   | 2         |
| 3D-printing [3]       | 0         | 2               | 2                   | 2         |
| State of research [2] | 2         | 1               | 2                   | 0         |
| Robustness [2]        | 1         | 1               | 2                   | 2         |
| Transportation [1]    | 2         | 1               | 2                   | 0         |
| Price [1]             | 3         | 2               | 2                   | 0         |
| <b>Total</b>          | <b>11</b> | <b>16</b>       | <b>27</b>           | <b>16</b> |

but also on Mars where achieving high temperatures might require a very high amount of precious energy. For example, extracting sulphur required a temperature of  $1100^{\circ}\text{C}$  and vacuum conditions. Moreover, the resultant paste has to be treated at high temperature (at least  $140^{\circ}\text{C}$ ) before and during 3D-printing for it to have acceptable properties, making it hardly suitable for 3D-printing in lab conditions. Hence, the overall score given to molten sulphur mixture is 11.

Portland cement is widely used on Earth in various structures. It mostly consists of calcium silicates ( $3\text{CaO} \cdot \text{SiO}_2$  and  $2\text{CaO} \cdot \text{SiO}_2$ ), with addition of aluminum and iron clinker phases. The required minimum ratio of calcium to silicon is 2.0 for a successful cement mixture, hence modification to the regolith powder or other way of introducing calcium into the mixture would have to be used (looking at Table 2.4). Processing of cement requires several steps and some of those steps require elevated temperatures, for example  $600^{\circ}\text{C}$  for calcining and  $1450^{\circ}\text{C}$  for sintering. This gives a score of 1 in processing. Cement is quite viscous, but does not have to be printed at high temperatures, hence the syringe outlet diameter can potentially be increased to facilitate printing, giving a score of 2 to it. Portland cement is deeply researched for applications on Earth, and some papers attempt to adapt it for Lunar construction, but the variation of properties with temperatures and pressures is not investigated much, giving it a 1 in state of research. It is known that Portland cement performs poorly in the conditions of extreme temperature swings and is weak in tension, while tensile strength is required to balance out the low pressure outside of potential habitat, earning 1 point in robustness. A large amount of processing equipment and at least water have to be transported from Earth, giving it a score of 1 in transportation. Finally, cement materials are quite cheap excluding the processing equipment, scoring 2 in price. Overall score is 16, which is higher than molten sulphur.

Geopolymer cement is flexible in the composition, with Sodium Silicate ( $\text{Na}_2\text{SiO}_3$ ) and water as basic components, with the possibility of adding strong bases (like sodium hydroxide or potassium hydroxide) for mechanical property improvement [33]. While Portland cement is based upon calcining and sintering processes, geopolymer cement is based upon chemical reaction. Processing of geopolymer mixture is very simple, as a portion of Sodium Silicate has to be dissolved in water and then mixed with the regolith powder, making a printable paste. This gives a score of 3 in processing, as it is fast and easy in laboratory as well as realistic on Mars. Printing a geopolymer mixture is not supposed to be challenging, as elevated temperatures are not needed and curing

occurs relatively fast, but the viscosity is unknown. It is assumed at this stage that viscosity can be manipulated through mixture composition, hence giving a score of 2 in printing. Some articles claim to explore the usage of geopolymer mixture in Lunar conditions, and present it as a usable alternative to Portland cement on Earth, awarding 2 points in state of research. Although geopolymer mixture theoretically can be cured in low temperature and pressure conditions, it is known that mechanical properties can suffer significantly because of it. However, robustness with respect to temperature swings of such mixture is better comparing to previously mentioned materials. Therefore, robustness earns a score of 2. It is indicated that a very small amount of binder mixture is sufficient to make a printable paste (2%), hence only a small amount of material has to be transported from Earth, earning this mixture a score of 2 in both price and transportation. The total score for geopolymer mixture is 27, which is the highest so far.

Polymeric binding, where regolith is simply an inclusion in a polymeric matrix instead of a reactive component, can potentially be a very viable option because of a large amount of various polymers like epoxies available. It should technically be possible to find a polymer with relatively simple processing conditions, good printing viscosity and acceptable robustness in Martian conditions. However, certain procedures and conditions regarding curing still have to be followed for any polymer to cure, and for evaluation printing properties more information has to be known. Hence, processing conditions, 3D-printing possibility and robustness earn a score of 2 each. Using polymers for Martian building application is merely a suggested concept, without particular ideas discussed, hence a 0 in state of research. Typically, polymer mixture is complicated to synthesize and requires water, which has to be brought from Earth. Also, polymeric building mixture would require a significant amount of polymer to incorporate regolith without losing too much of mechanical properties. Therefore, both transportation and price get 0. Total score of polymeric option is 16 points.

As it can be seen, geopolymer binder has scored the highest points by a significant margin because of easy processing and promising literature study information. While Sodium Silicate and water are the base components of geopolymer binder, it is possible to use a strong base to improve mechanical properties of resultant mixture. However, for the reasons of safety and time constraint, only a base mixture is going to be used in this research. Figuring out an optimal geopolymer mixture composition would introduce too many variables to handle efficiently, and would steer this research away from the main questions. Therefore, the final mixture chosen from this trade-off is Sodium Silicate solution in water of various mixing ratios.

### 3.3. Pure Material Properties

In granular form, Sodium Silicate ( $Na_2SiO_3$ ) is a white solid powder with particle size of approximately 0.5-1 mm. The powder has melting point of 1088°C and density of 2.61 g/cm<sup>3</sup> at 20°C. Due to a high melting point, there is no need to be cautious of temperature when it comes to storage con-

ditions, except for the fact that the powder is corrosive towards aluminum and zinc. Additionally, it should be kept away from drinking water and food to prevent contamination, and acidic environments due to alkaline nature of the substance.

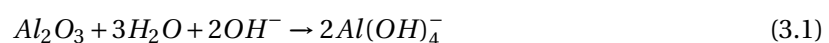
This powder is soluble in water, but the solubility highly depends upon the ratio of powder to water and water temperature. The solubility in this context is meant to be complete when the solution is fully transparent, and no undissolved powder particles are visible. Between 25°C and 80°C, solubility varies between 22.2 g per 100 ml (18% concentration) and 160.6 g per 100 ml (61.6% concentration). Time is also an important variable when making the binder solutions, because the amount of time required for dissolution increases as temperature decreases and desired concentration increases. To reduce the time required for the solution to form, stirring is used by the means of a heated magnetic plate and a stirring pill. Stirring conditions applied for the binder mixtures used in this report are 80°C and 360 rpm stirring rate. Depending upon desired concentration, mixing time varied between 5 minutes and 20 minutes at the noted stirring conditions.

While temperature determines the theoretical highest amount of powder that can be dissolved in a solution, in practice there is another aspect that puts a restriction upon the binder concentration. When the solution is formed, high-concentration solutions start forming crystals after a certain period of time. For instance, solution of 55% Sodium Silicate to water ratio stayed in a fully dissolved form for only 3 minutes, so it had to be used immediately to ensure consistent paste properties. During preliminary testing phase, mechanical properties of samples made with pure solution were considerably better than the ones made with murky solution. Solution of 50% Sodium Silicate to water ratio had a 12 minutes processing window, which allowed for more convenient and consistent sample making.

### 3.4. Chemical Properties

Geopolymer reaction consists of five major steps, which are schematically shown in Figure 3.1. For this reaction to initiate, an aqueous alkaline medium (hydroxide or silicate) has to be combined with solid component that includes aluminates and silicates, preferably in powder form. Upon mixing these two components, in this case regolith powder and liquid binder solution, the reaction initiates.

Dissolution is a stage where aluminosilicate particles from regolith powder start dissolving in alkaline medium, provided by sodium silicate solution. As the result of this phase, monomers of aluminates and silicates are formed. This reaction step consumes water to produce the reactive particles. General formulae of this hydrolysis reactions for aluminates and silicates, where only mass and charge balances are taken into account, follow as:



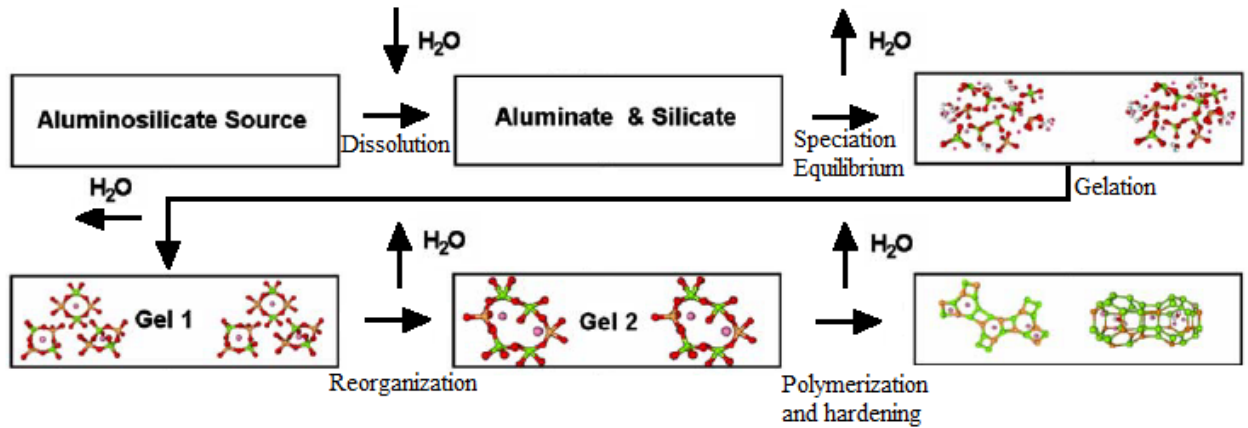
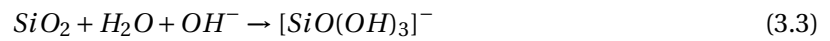
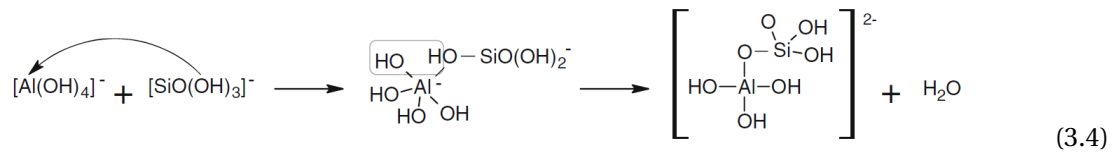


Figure 3.1: Schematic representation of geopolymerization reaction [1].



Speciation equilibrium, also described as solution saturation in this case, is reached faster with higher pH values. As solution becomes saturated with the particles from previous step and subsequently oversaturated, aluminosilicate particles combine with each other to nucleate and form small oligomers. During this process, water is being condensated. It can either evaporate if the reaction happens close to the surface, or it stays trapped within the material bulk in pores. An example of forming a dimer between  $\text{Al}(\text{OH})_4^-$  and  $[\text{SiO}(\text{OH})_3]^-$  is shown in the following equation:



Gelation happens as more and more monomers combine together into oligomers, and so mixture becomes less and less liquid. This forms a what is referred to as Gel 1 phase, which consists of a large amount of small oligomers. These oligomers continue to react with each other, releasing water into the system, but eventually because of restricted mobility, no nearby connections can be established anymore. At this point, formed oligomers begin to reorganise in order to form more connections within the polymeric network. At the same time, as aluminum particles dissolve considerably faster than silicon ones, the silicon groups continue to dissolve and participate in the polymerisation process. This process continues to harden the material bulk, forming a more stable in shape

Gel 2 phase. The last stage of the polymerisation reaction (with Potassium instead of Sodium, which also can be used for this purpose) is shown in Figure 3.2. The speed of this phase depends upon ambient conditions and initial component compositions. For example, unfavourable balance between aluminum particles, silicon particles, alkaline medium and water might lead to gel not even forming in the first place.

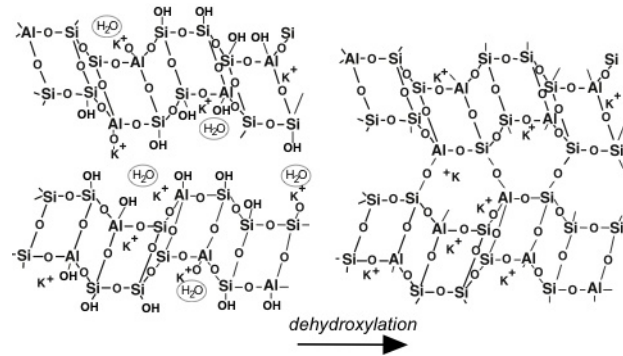


Figure 3.2: The last step of forming a 3D polymeric network within geopolymer reaction (with Potassium instead of Sodium) [2]

It should be noted that varied outlined reaction steps occur concurrently in different locations of the bulk, and do not progress strictly in order in whole the bulk [34]. For example, initial gel precipitation starts when the solution in a particular location reached saturation. However, other locations can be still reorganizing to achieve that. This can be viewed from a microscopic image in Figure 3.3, where in some locations the material still flows to reach destination (mostly on the right), while other locations have reached saturation and started gelation phase (mostly on the left). Hence, it is important to provide sufficient time for the mixture to complete the reaction process before using the product, as the overall reaction progression can vary in different bulk locations. Also, varying reaction progression between the regions can introduce inhomogeneity in the bulk, as less links between the regions can be formed in the end.

### 3.5. Reaction Variations

For the purpose of this project, a simple Sodium Silicate solution is going to be used in combination with regolith. However, both regolith and binder can potentially be enhanced to improve the mechanical properties of final product [35]. Besides the curing conditions, the properties of geopolymer concrete depend upon the solution pH value, ratio between silicon and aluminum, and degree of powder processing.

When it comes to degree of regolith powder processing, smaller particles allow for faster overall dissolution of aluminosilicate particles in aqueous medium. The powder used in this report was preprocessed into fine size particles before packaging and shipping, meaning the dissolution during the mixture creation is fast and homogeneous. However, in real application conditions, regolith

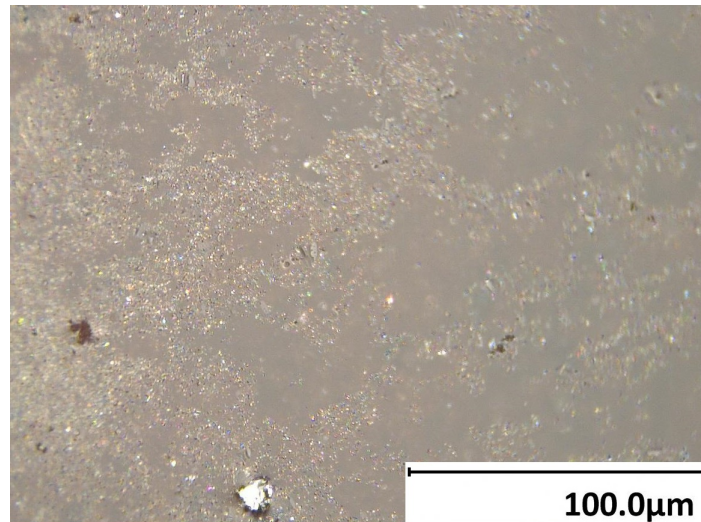


Figure 3.3: **Microscopic image of a mixture surface during saturation and gelation phases (x1000)**

powder on Mars might contain very large particles together with small ones, increasing not only the dissolution speed, but introducing further reaction speed discrepancy between the various regions in the material bulk. This might lead to non-homogeneous final properties, which is not good for overall mechanical properties. This is easy to bypass however, as a grinder machine can be used in order to reduce the overall particle size, potentially together with sieving machine.

Optimally, the binder should include a strong base as one of the components, for example Sodium hydroxide  $NaOH$ . It serves multiple purposes in the geopolymer mixture, namely introduces easily accessible hydroxide particles  $OH^-$  which can be incorporated in the monomers, increase alkalinity of the mixture speeding up the reaction, and also act as a catalyst during the gelation phase. However, for the purpose of this project it was decided to omit the usage of hydroxide. First of all, working with a strong base is more dangerous, and considering experiments with 3D printing where pressure is involved are required, mishandling the solution could potentially have negative influence on the printer and surroundings. Also, a large amount of samples is planned to be made at the same time, and making solution with one soluble material is faster and more convenient. Adding a base into the picture also would introduce another variable in the resultant sample matrix, yielding less useful information in the end due to time restrictions. Overall, using a simpler solution provides better baseline results for figuring out the dependency on the main variables of the reaction: temperature and pressure.

Expanding on the previous point, higher alkalinity does not always directly improve the resultant mixture properties [36]. In fact, high alkalinity induces the formation of  $[SiO_2(OH)_2]^{2-}$  (Equation 3.2 over  $[SiO(OH)_3]^-$  3.3). The former particles tend to form smaller oligomers with  $2Al(OH)_4^-$  and halt further polymerisation, while the latter allow for more links to be formed and hence increase the size of resultant polymer. This means that the balance between  $[SiO_2(OH)_2]^{2-}$  and  $[SiO(OH)_3]^-$  particles directly impacts mechanical properties of the formed geopolymer cement, which in turn directly correlates to the alkalinity of the solution. This is one of the reasons why typ-



ically a combination of a base and a silicate is used over a pure hydroxide.

Another component property that strongly affects the mechanical properties is the ratio between silicon and aluminum in the mixture. Mechanical strength, porosity and elastic modulus all depend upon this ratio. If the Si/Al ratio is low (below 1.4), the microstructure of resultant cement is reported to be highly porous and inhomogeneous, resulting in inferior mechanical properties. The ratio above 1.9 shifts the particle balance in another direction, lowering the mechanical properties as ratio goes further up. Between ratios of 1.65 and 1.9, the porosity is low and material bulk is largely homogeneous, which translates into high mechanical strength and elastic modulus. Such behaviour is explained by chemical balance between the particles, where skewed particle ratios result in high amount of unreacted particles, creating defects inside the final product.

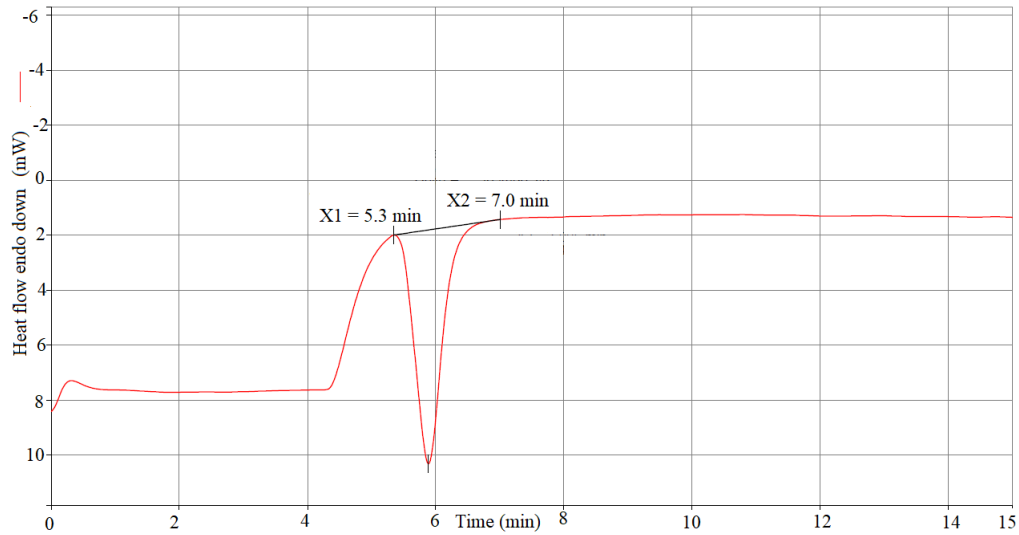
While these parameters are important when it comes to geopolymer cement formation, they are not considered in the context of this investigation. The aim of the project is to utilize Martian regolith as it is, and a certain bulk of regolith simulant with given particle size and composition was used for this purpose. Making changes in the regolith composition would translate into a higher amount of work when it comes to real application, and would introduce too many new variables to modify. Similar reasoning goes for the binder solution enhancement, where a new solution component would complicate the solution creation and balancing process, and also would make the research more dangerous for the surroundings.

### 3.6. Curing Reaction in Practice

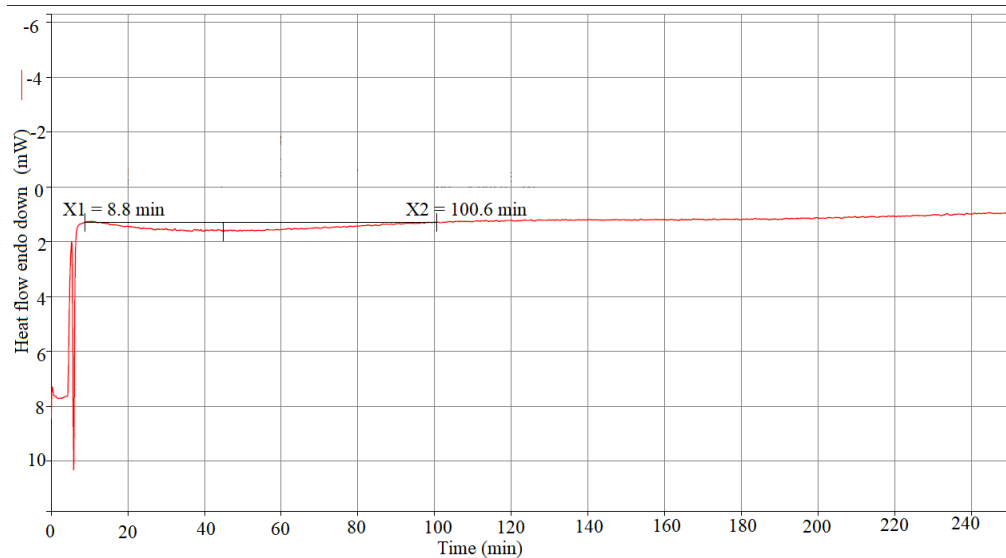
To investigate the curing reaction properties, DSC (Differential Scanning Calorimetry) analysis was conducted by curing the samples with the same composition and various temperatures. These temperatures are those at which actual samples are going to be cured. This DSC analysis allowed for a better estimation of time that initial gelation and final hardening takes, which contributed to the optimal sample processing sequence. Removing the sample after the shape is established, but before complete drying and hardening happens allows for easy removal of the sample from the mould without the risk of damaging it, especially in the case if the sample is already weak because of sub-optimal composition.

DSC experiments were conducted for the same temperatures that were selected for curing: 2°C, 23°C and 60°C. It was expected that low-temperature cure would take a long while, hence the measurement was conducted over night [37]. DSC method used for this measurement consists of decreasing the temperature from room conditions to 2°C at the rate 5°C per minute (default rate), holding the sample at 2°C for 12 hours, heating up back to room temperature at the rate 5°C. From the resultant plot, the reaction seemed to be completed within 100 minutes from the start of experiment, which can be explained by a very small sample size (approx. 11 mg). After 100 minutes, the curve has a shape of a straight horizontal line. Figure 3.4b covers the part of the result plot which

contains the reaction space. As it can be seen, the second part of curing (hardening) lasted for 92 minutes. The first part of cure happened considerably faster as it can be seen in Figure 3.4a, which covers the very beginning of experiment. The increase in heat flow happened in under 2 minutes, which is quite fast.



(a)



(b)

Figure 3.4: DSC plots for curing the sample at  $2^{\circ}\text{C}$ , separated into two different time frames for clarity. (a) The first gelation step (time period 0 to 20 minutes). (b) The second gelation step (time period 0 to 250 minutes).

The second DSC test was conducted simply by holding the sample at room temperature of  $23^{\circ}\text{C}$  for 4 hours. The result of this measurement, from the start until the point of curve straightening, is shown in Figure 3.5. Unlike in the case with low temperature cure, the first gelation phase starts almost immediately upon loading the sample in the DSC apparatus, as the beginning of the drop is

at 1 minute. Seemingly the first phase here lasts longer than in the case with low-temperature cure, namely for 19 minutes. After that, the second phase lasts for approximately 1 hour. It is important to note that the sample size in this case was approx. 21 mg, which could explain the length of the first phase.

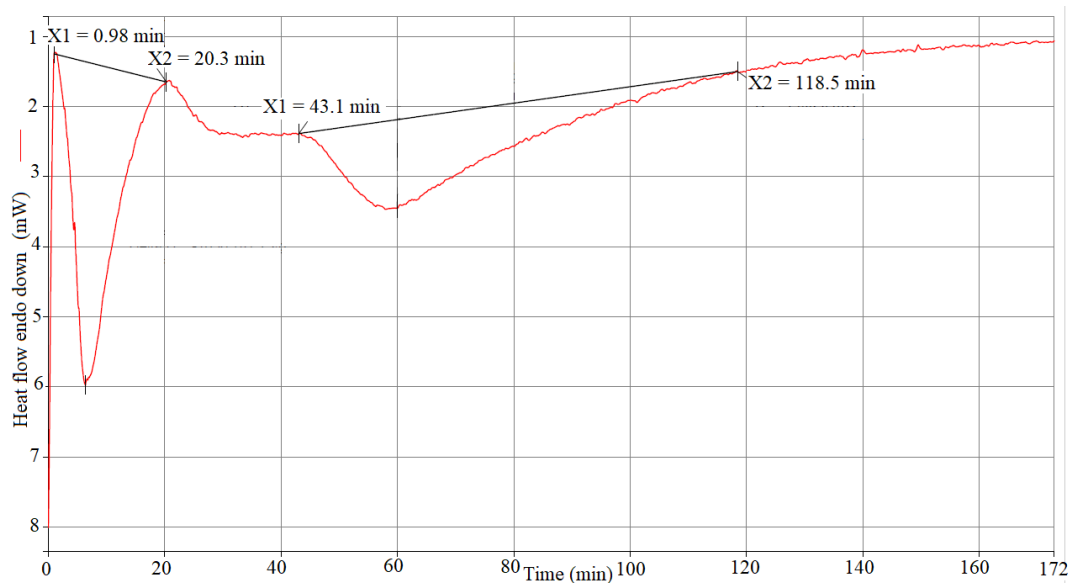


Figure 3.5: Complete DSC plot for curing the sample at 23°C, including analysis of both cure steps.

Knowing that high-temperature cure occurs considerably faster, the selected method was heating up the sample from room temperature 23°C to 60°C at a standard rate of 5°C per minute, holding it for 2 hours, and dropping the temperature back to room conditions. As it can be seen in Figure 3.6, the complete reaction was done in under 20 minutes. The first gelation step ended within 5 minutes, while the second gelation phase lasted for 13 minutes only. Sample size in this scenario was approx. 13 mg.

From these results, it is clear that the second gelation phase, or hardening of the mixture, happens considerably faster at higher temperatures. Indeed, knowing the reaction, in this phase oligomers rearrange themselves in order to find more available connections and form a complete 3D network, where mobility plays crucial role. For the first phase, however, this dependency does not seem to be the case. Looking at the beginning of DSC results for low-temperature cure, it can be noticed that the curve starts with a straight line, while the other two plots start with a sharp rise. It could be the case that because 2°C cure started at room temperature and then the temperature dropped, the heat flow change from the temperature drop cancelled out the curve part related to the first stage of the cure. Regardless, looking at the reaction it is clear that the first gelation stage, where small oligomers form, depends more upon the concentrations of necessary components and alkalinity of the mixture, and temperature is not as important due to assumed homogeneous distribution of the components. The reaction there can occur straight away, without much movement necessary.

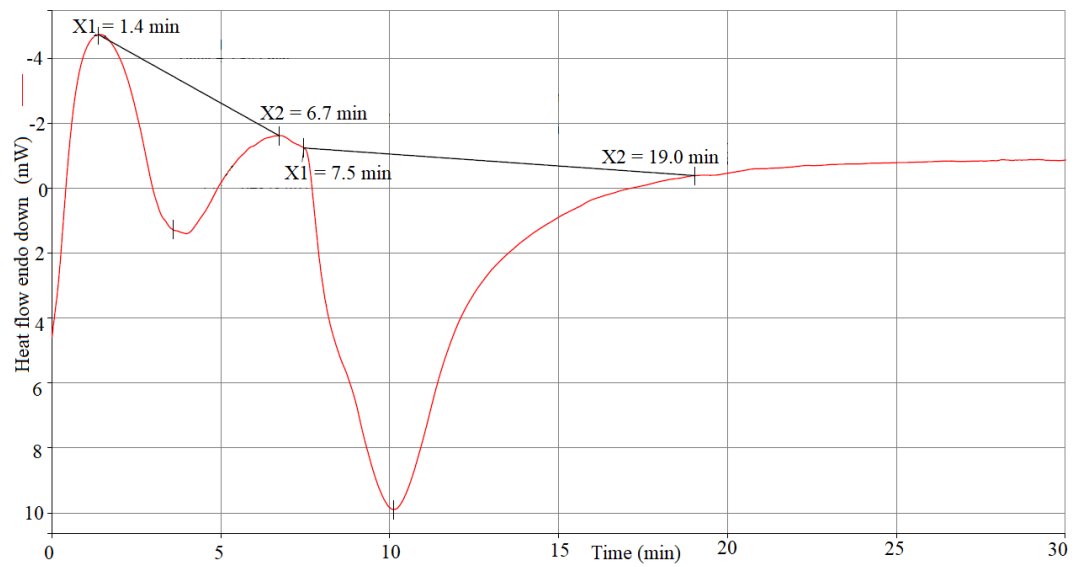


Figure 3.6: Complete DSC plot for curing the sample at 60°C, including analysis of both cure steps.

# 4

## Moulding Process

Although the research is supposedly concerned with 3D-printing the regolith paste, moulded samples serve as a reference point in result evaluation. Through moulding, it is more convenient to see the dependency of mechanical properties of cured samples on ambient conditions due to lower number of processing parameters. Also, it is easier to change the paste compositions when it comes to moulding, as varying thickness of the paste has a very high impact on printing process.

Section 4.1 presents designing and preparing a suitable set of moulds which can produce samples of desirable dimensions. Section 4.2 explains the sample preparation procedure, including post-processing. Section 4.3 shows all the chosen paste compositions and curing conditions, with comments on why those particular values were selected.

### 4.1. Mould preparation

The selected mechanical test for regolith cement samples is three-point bending test, for which the samples require to have a shape of rectangular block. While for most cements compressive test is preferable, it requires a more complicated to produce shape (a cylinder). Cylindrical shape would require higher amount of material per sample, and the amount of surface touching the mould walls would be considerably higher. This, in turn, would make the sample removal process significantly more destructive for the sample as compared to rectangular block sample. Besides, for application on the surface of Mars, tensile strength is as important as compressive strength, as the pressure inside the habitat has to be increased to a value that is comfortable for human activity, while outside pressure is very low. This pressure differential inflicts tensile stress upon the structure in addition to compressive stress that buildings endure.

According to the three-point bending test specifications, the dimension for the sample should match the following proportions [38]:

$$l = 6t, w = 2t, \quad (4.1)$$

where  $t$  is the sample thickness,  $w$  is the sample width, and  $l$  is the sample length. Based upon these proportions and preliminary mixture property investigation, selected thickness is  $t = 5$  mm. This gives  $w = 10$  mm and  $l = 30$  mm. Samples smaller than this have too high of a risk to be destroyed during the mould removal because of low thickness, and larger samples use too much material and require longer time to cure, which is an important factor because of a large amount of samples planned to be produced.

Sample moulds were 3D-printed using PLA (polylactic acid) material. Both schematic drawing of mould parts and printed result are shown in Figure 4.1 To speed up the sample creation process, 12 such moulds were printed.

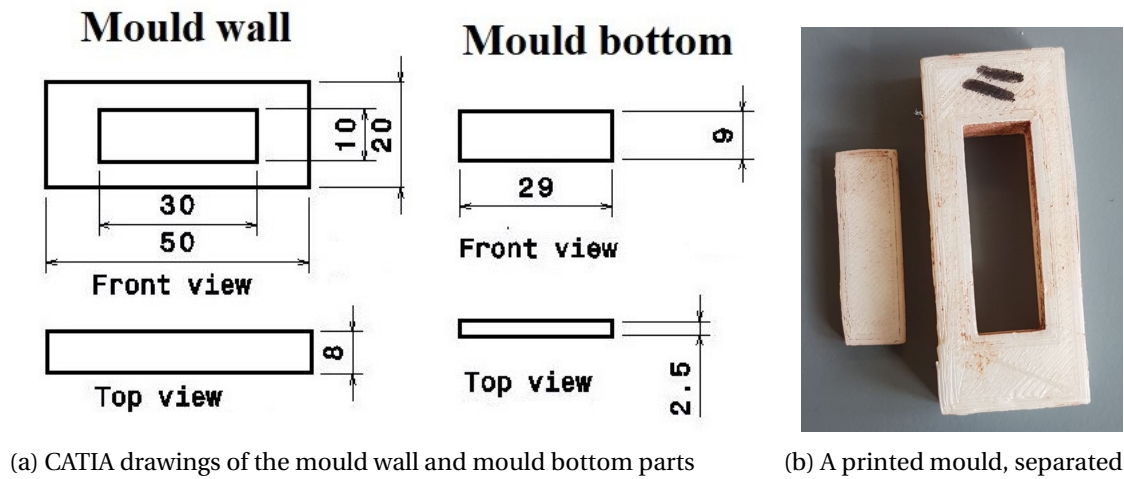


Figure 4.1: The appearance of a mould in the drawn form and the printed form







The idea behind such mould design is to pour the mixture into the assembled mould, and then carefully push the sample out using the detaching bottom part. If the sample is connected to the walls strongly, like in the case with high-temperature cure where the mixture expands, a thin razor can be moved in between the sample and mould wall. From the drawing, it can be seen that the dimensions of the bottom part are smaller than the cavity of the walls. This is made to account for printing imperfection, and also to ease the removal process, as a more loose bottom is safer to push without applying too much force.

## 4.2. Sample Preparation

Before preparing the moulded samples, certain equipment has to be gathered for fast and efficient moulding. This equipment includes: necessary amount of moulds (numbered), matching amount of cups, laptop with an Excel sheet that concerns properties and calculations regarding current samples, a pipette for binder deposition, a stirrer, scales, a bulk of regolith and binder solutions. An Excel

sheet contains a matrix with sample numbers to correlate them to a specific numbered mould, solution and regolith concentration, calculation field that shows required amount of binder solution for given regolith weight, and space for mechanical testing results to be filled later. Visualized steps of producing a moulded sample are presented in Table 4.1.

Table 4.1: The steps of making a moulded sample.

|  |  |  |
|--|--|--|
|                             |   |    |
| <p>Step 1:<br/>Weight an empty cup<br/>Reset weight to 0</p>   | <p>Step 2:<br/>Add regolith powder<br/>to the cup (2.5-2.8 g).<br/>Insert the weight into Excel<br/>formula.</p>                     | <p>Step 3:<br/>Add binder as<br/>calculated by Excel<br/>sheet. Here, 65% regolith<br/>sample is being made.</p>   |
|                           |   |    |
| <p>Step 4:<br/>Thoroughly mix<br/>the sample. High regolith<br/>content mixtures take<br/>longer to mix.</p> | <p>Step 5:<br/>Pour the mixed paste into<br/>a mould. It should<br/>overflow from the mould<br/>to ensure consistent dimensions.</p> | <p>Step 6:<br/>Wait until the sample is dry.<br/>Remove the sample from<br/>the mould when it is<br/>solidified. In the image, the<br/>left sample is not good as<br/>it is too thin, hence mixture<br/>should be overflowing when<br/>preparing the sample.</p> |

The range of regolith powder weight was determined during preliminary testing. Regolith quantity smaller than 2.5 g generates the amount of mixture that is not enough to overfill the mould. This leads to a sample that is too thin, like shown in the Step 6 of the Table 4.1 on the left. More than 2.8 g of regolith makes too much powder, which not only wastes the material, but also fills the mould with leaving some mixture in the mixing cup, risking inconsistent mixture concentration. The mixture is combined using a stirrer, and while low regolith concentration mixtures (60%) are combined fast and easily due to high amount of liquid (within 3 seconds), high regolith concentration mixtures (70%) have to be mixed for longer (30 seconds), as the amount of liquid is just enough to cover all the powder. The viscosity variation is very high depending upon regolith concentration, which is a useful observation when it comes to printing.

After pouring the samples, a plate with the filled moulds is stored for curing. Samples cured at low temperature are stored in refrigerator, samples for cure at room temperature and pressure are stored on the laboratory table, while samples for cure at low pressure and high temperature are stored in the oven with corresponding temperature set beforehand. Low pressure is reached after placing the samples in the oven. During the second curing stage, while the samples are still soft but have a set shape, they are removed from the moulds by pushing the bottom mould part through. This way, they are easier to remove without damaging the sample. Also the exposure to ambience is more even for the rest of the curing time, drying the samples out more equally. When the samples are completely dry, which depends upon curing temperature, they are placed back into the mould and the excess material on top is grinded away to ensure equal dimensions across the samples. Finally, each sample is stored in a small plastic bag marked with the sample type and number for further mechanical testing.

### 4.3. Curing conditions of moulded samples

For the purpose of mechanical evaluation of the selected binder/regolith combination, multiple parameters have to be varied to generate a better overview of the properties. In the end, four parameters are selected: temperature, pressure, binder concentration, and regolith-to-binder ratio. Samples were made in bulks of 12, and hence this amount of moulds was printed.

First of all, room condition cure is very simple to perform, as no additional equipment is required. Basic 3D-printing samples therefore are also printed in room conditions. Because of this, room condition cured samples serve as a baseline for mixture property evaluation, and more samples are created at these conditions than at other ones. The sample matrix for room conditions cure is shown in Table 4.2.

Regarding the binder and mixture concentrations, there are restrictions that define the boundary conditions. When it comes to regolith concentration, at 70% the mixture is hardly mixable, and it takes significant effort to get all the powder covered in liquid. During the preliminary testing, al-



Table 4.2: **Sample composition matrix for curing in room conditions.**

| Regolith concentration [%] | $Na_2SiO_3$ concentration [%] | 30 | 35   | 40 | 45 | 50 | 55 |
|----------------------------|-------------------------------|----|--|----|----|----|----|
|                            | 60                            |    | 2 samples for each condition were made (36 samples in total) |    |    |    |    |
| 65                         |                               |    |  |    |    |    |    |
| 70                         |                               |    |  |    |    |    |    |

ready at 72% regolith not all powder could be possibly covered by the binder, rendering this ratio too high. At 60% regolith concentration however, the mixture forms very easily within a couple of stirs, and all the powder gets suspended in liquid. During the preliminary testing even lower concentration of 55% regolith was tried, but a lot of cracks were observed after the curing process and overall mechanical robustness resulted to be very low. Besides, in real applications, as high regolith concentration as possible is desired for reduced transportation costs. Hence 60% concentration is deemed the lowest to be investigated.

The binder concentration boundaries were determined through binder solubility information and preliminary testing. As indicated in Section 3.3, at 80°C highest concentration possible is 61.6%. However, in practice the solution with concentration of 60% was not completely forming after 30 min of stirring at 80°C, and going to higher temperatures would cause the liquid to evaporate too fast, skewing the resultant concentration. Solution of 55% concentration was able to be formed, but it did not last in completely transparent form for longer than 3 min. This was the highest solution concentration boundary. At 30% concentration, the preliminary testing samples were mechanically extremely very weak after curing, hence it was selected as the lowest boundary for the tests.

After the mechanical testing of samples cured at room temperature, the binder concentration of 30% was eliminated because of insufficient strength comparing to higher concentrations. 55% concentration binder was also eliminated because of both fast solution crystallization and reduced mechanical properties comparing to 50% solution. As fast crystallization produces unreliable results, it was decided to skip this binder concentration in further experiments. For further samples, only 1 sample per situation was produced, as making them for such large amount of situations took a lot of time. The resultant sample matrix is present in Table 4.3.

Table 4.3: **Sample composition matrix for curing other than room conditions.**

| Regolith concentration [%] | $Na_2SiO_3$ concentration [%] | 35 | 40  | 45 | 50 |
|----------------------------|-------------------------------|----|---|----|----|
|                            | 60                            |    | 1 sample for each combination (12 samples in total) |    |    |
| 65                         |                               |    |   |    |    |
| 70                         |                               |    |   |    |    |

Overall summary of temperature and pressure conditions with respective cure locations is shown in Table 4.4. As vacuum ovens are not suitable for providing low temperatures, it was only possible to perform low temperature cure in refrigerator, where pressure is 1 bar. Samples cured at room conditions were left at the laboratory table, hence there probably was some small temperature variation. The rest of the samples were cured in the vacuum oven.

Table 4.4: Temperature and pressure variation selected for the sample creation.

| Pressure<br>[ bar] | Temperature<br>[°C] | 2  | 23   | 60              |
|--------------------|---------------------|--|--|-----------------|
| 1                  |                     | Table 4.3, refrigerator, with this temperature setting available | Table 4.2, better baseline for evaluating printed samples is required. Room conditions | Table 4.3, oven |
| 0.1                |                     | - (no available equipment)                                       | Table 4.3, oven  | Table 4.3, oven |
| 0.01               |                     | - (no available equipment)                                       | Table 4.3, oven  | Table 4.3, oven |

# 5

## Additive Manufacturing Process

Moulded samples provide a large variety of data regarding mixture composition properties and influence of ambient conditions. While some conclusions about the mixture viability can be made from the moulding process, it is useful to see how such mixture can perform at similar conditions, but printed instead.

To produce printed samples and evaluate their properties, the principles of the obtained 3D-printer are discussed in Section 5.1, also with available settings in Section 5.2. Based on these settings, a printing program has to be set up that satisfies the requirements for printed samples, as shown in Section 5.3. Section 5.4 investigates the resultant printed samples. Furthermore, the printer can potentially be improved for the purpose of this research by adding pressure and temperature variation functionality. Section 5.5 covers the Martian ambient conditions that are to be expected and should be simulated, while Section 5.6 explores on the plan to achieve those conditions.

### 5.1. Printer Characteristic

The printer used for this project is Techcon Systems Automated Dispensing Robot model TSR2301. Primarily used for dispensing fluids, it can operate within 3 axis, being a 3D-printer. As shown in Figure 5.1a, x-axis movement is performed by a moving syringe mounting head, z-axis movement through the moving plate upon which the material is deposited, and y-axis movement is done through syringe holder extension. Deposition of the material can be done through manual positioning of the coordinates using the printer keypad together with the pressure control unit, but it is not precise and hence is not recommended. Deposition programs can be written and fully customized using the teaching pendant (Figure 5.1b), which is connected to the printer and is capable of receiving commands from user and sending them to the printer. Regulation of the pressure and time for material deposition process is done using a fluid deposition control unit shown in Figure 5.1c, which is directly connected to the syringe with material in a form of syringe cap [3].

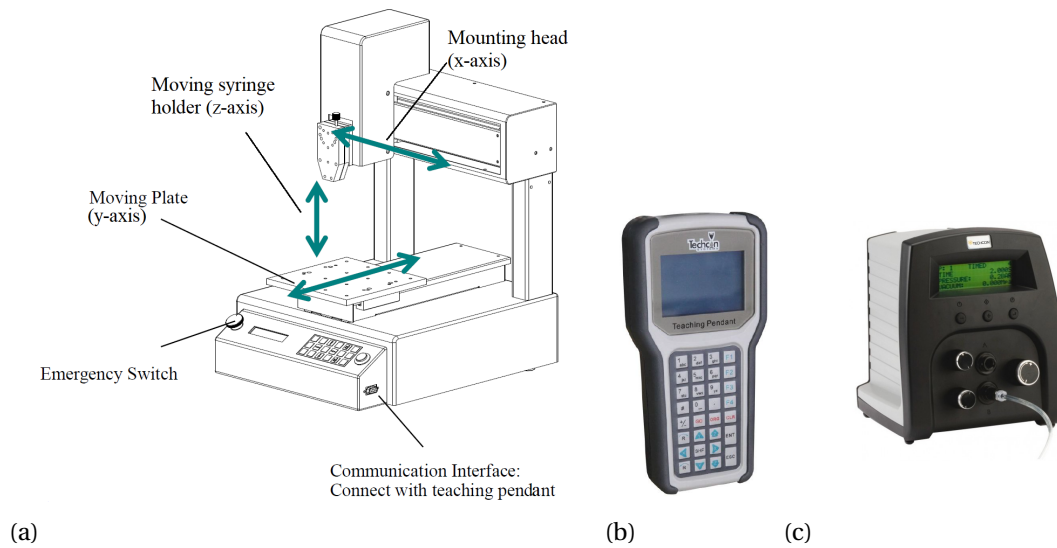


Figure 5.1: **Key components required for the 3D-printing process. a) Schematic representation of selected printer model with key components indicated [3]. b) Teaching pendant [4]. c) Digital fluid dispenser, responsible for pressure control [5]**

In order to operate a printer, a program has to be written. In this program, the user specifies the shape which consists of 3D coordinates along which the syringe head moves with respect to deposition plate, syringe movement speed, dispense time, retraction height and lift height. A more elaborate description of pendant programming capabilities is given in Section 5.2. The program is then communicated to both printer and fluid dispenser unit. Fluid dispenser unit has a setting which determined both pressure when depositing the material and optional suction to keep the material inside the syringe when the printing is halted. It also has an option to perform manual pressure pulse which is useful for testing the material properties without writing a program. When a program is being executed, printer moves the syringe head in a programmed pattern, while fluid dispenser unit provides pressure that pushes the syringe content out [4].

Operating conditions for the printer lie within 0-40°C, which excludes the use of high-temperature materials and processing conditions during the printing process. However, it allows for simulating lower temperature conditions, for example between 0-20°C like how it is in warmer regions of Mars during the day. Overall, this temperature restriction does not allow for a wide range of temperature to be tested using the current printer in the original configuration. Examples of such experiments include high-temperature printing, which combines looking at the behaviour of the paste during deposition and curing conditions, and simulating the Martian day-night cycle to see how the cure proceeds in varying temperature conditions. Such experiments can potentially be done by printing the sample in allowed temperature conditions and subsequently relocating the sample into an oven/refrigerator, where the cure at desired conditions can take place. However, this experimental setup does skew the results, as the beginning of the curing stage, that happens upon deposition, is as important as subsequent stages, as the mixture starts to form oligomers and gelate quite fast (within several minutes).

The selected printer model can be used as a binder deposition 3D-printer. Having no extra processing tools like for example a Fused Deposition Modeling (FDM) printer would have, it is severely limited by the viscosity of the sample, especially combined with the temperature restrictions and syringe design with a relatively small outlet (3 mm outlet diameter of syringe supplied by the manufacturer). In this particular scenario, the printer is used as a material deposition printer, but without extra processing tools that are usually present when working with such printer (filament melting mechanism like in fused deposition modeling printer or curing laser like with selective laser sintering printer). In order to simulate Martian conditions, extra processing is not required, however for further development of Martian 3D-printing material additional modifications to this printer should be considered. If successful, such modifications might be applied in a real scenario.

## 5.2. Printer settings

The printing volume in along which the syringe outlet can move is 300 mm in x-direction, 300 mm in y-direction and 100 mm in z-direction. Using the test option in the teaching pendant, it is easy to see which coordinate responds to which location on the deposition plate, which allows for simple calculation of programming input. During the programming, it is possible to select preset deposition shapes such as dots, lines, polylines with round edges, circles and even arrays of shapes. Coordinates are measured in millimeters from the starting location, making it convenient to pre-plan the desired shape in for example Excel and then input the coordinates. Teaching pendant manual provided with the hardware has instructions for programming each included shape.

Patterning speed and dispense pressure are the deposition parameters that are related to each other together with syringe outlet diameter. The patterning speed can be specified for each program step and determines the speed of printer head movement along the program steps. Dispensing pressure is a setting on the fluid dispenser unit, and is limited by the pressure available in inlet pressure, up to 6.9 bar specified by the machine settings. These three parameters (patterning speed, dispensing pressure and nozzle diameter) are crucial when determining the speed of printing and line thickness. Low pressure combined with low deposition speed can produce fine uniform lines, as the deposition is done in a more natural way, while high pressure and high speed can perform the print fast and create a thick line. Viscosity and pressure-induced behaviour of the material are of utmost importance when determining the operating pressure and syringe diameter. High viscosity and small outlet diameter require higher pressure levels to get the material out of syringe, while low viscosity and large outlet result in material being ejected too fast, making inconsistent turbulent flow. When the optimal and consistent flow of material is ensured, pattern speed can be adjusted for each particular program step to ensure required deposition line thickness.

Lift and retract speed and height are the parameters that affect the syringe movement between depositions. These should not be confused with retraction speed and height in FDM printers, which

are related to drawing the filament back inside the nozzle between deposition cycles to prevent oozing. In this case, lift height and speed determine the nozzle home location after the printing process is complete, while retract speed and height determine the syringe movement between the programmed steps. Normally, the lift height is set at the highest location along z-axis, so after the printing cycle is complete there is plenty of space to remove the sample. The speed of lift is determined by the machine movement speed and cannot be programmed for a particular pattern. The general machine setting has to be changed instead. Retract height and speed can be specified for each program step. Overall, retract height and speed need to be specified to avoid collision with material that is already printed and also prevent unwanted oozing, as if the syringe moves between locations too close to the printed material, extra material might get deposited due to surface tension. In some situations however, this surface tension is wanted in order to ensure uniform deposition, especially if the viscosity of the mixture is high, like in the case with this project. Slow retraction close to the printed sample between printing steps can make the paste to be deposited in one continuous line.

The last discussed parameter related to the printer is "feed on delay". This option prevents the inconsistency in the beginning of printing process, when the material placed inside the syringe has not yet reached near the very outlet. Beginning the printing straight away results in the start of the pattern not being printed out, as the material is still moving towards the outlet in the first moments. Feed on delay allows for a short pre-load of the material, getting it to the outlet. If it is done for too long however, some material can already exit the outlet before printing process actually starts. Hence, the delay duration should be adjusted through trial and error, and it is easier to adjust if the material is of uniform viscosity.

### **5.3. Modifications to the printer and program**

As the printer is designed to operate with binders, which have relatively low viscosity as compared to the paste used in this project, multiple issues arose when trying to design a program suitable for printing regolith paste. This section deals with how these issues were resolved and what effects these solutions had on the final samples.

First of all, the viscosity of the paste is of vital important when it comes to printing, especially with such limited outlet diameter. Low viscosity mixture (as determined experimentally, 65% regolith and below) did not hold the shape upon deposition at all, flowing all over the build plate. Mixture with the lowest possible regolith ratio that could hold the programmed shape was the one with 66% regolith concentration, which determined the lower boundary for printing. Because of rapid viscosity change with respect to regolith ratio, going up to 69% regolith content resulted in a paste that was too thick to be printed even with the largest syringe diameter possible (7 mm), which will be discussed further in this section. Hence, the regolith ratio range which was possible to be printed was severely limited by the printer design.

The outlet diameter of printing syringe provided by manufacturer peaked at 3 mm, which is way too low for current application. Through this syringe diameter, even the paste of 60% regolith concentration required too high of deposition pressure, and deposited material was too liquid to hold the programmed shape. Because of this, the syringe was redesigned in order to achieve two goals: increase syringe outlet diameter, and increase the slope inside the syringe, as horizontal bottom of the syringe causes the material to be pressed against it and cure under pressure instead of being pushed into the outlet. For visual comparison, original syringe is compared to the redesigned syringe in Figure 5.5. While the geometry of the upper part of the syringe had to stay the same in order to accommodate the cap, which should be fit tight to avoid pressure escaping, the bottom part was redesigned. The limitation for bottom part redesign included a 11 mm hole on a mounting unit, through which the end of the syringe had to fit in order to be fixed properly with a screw. Non-fixed syringe can potentially wiggle during printing, distorting resulting deposition line. The slope inside the syringe was changed such that the material can flow into the outlet with less resistance instead of being pressured into the lowermost walls. The syringe was printed using PLA material, which is quite weak when it comes to withstanding the pressure, hence the walls of the syringe were made thicker than in original design, having a minimum thickness of 1 mm at the nozzle and 1.75 mm in the middle part of the syringe.

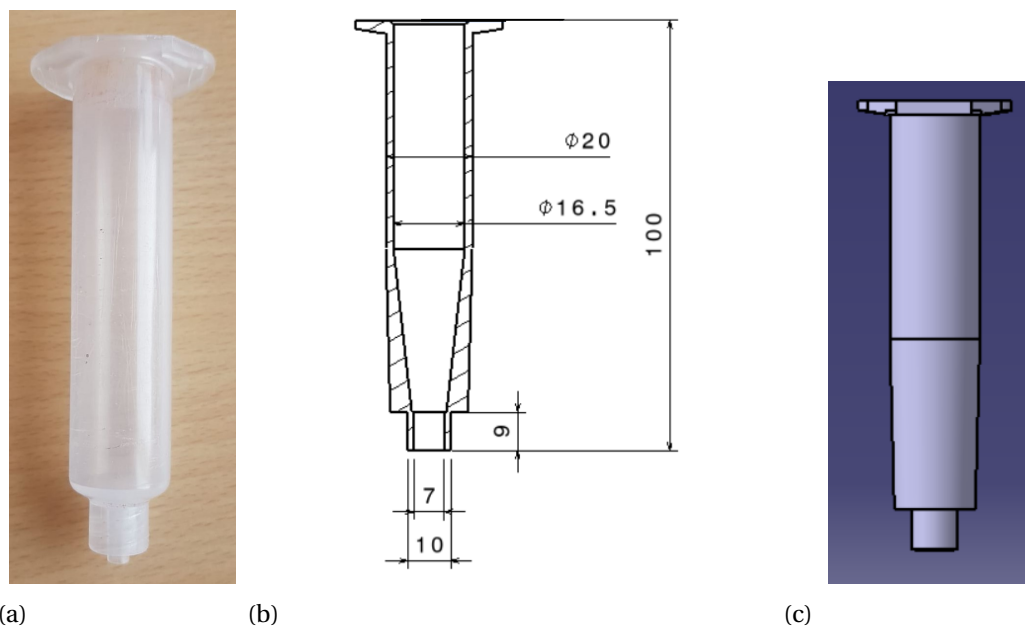


Figure 5.2: Syringes used for 3D-printing with the provided printer. a) Manufacturer design, unsuitable because of narrow outlet. b) Redesigned syringe, with largest outlet possible in current situation. c) Rendering of the redesigned syringe

The issue of rapid mixture curing under pressure complicated the printing process significantly. Although syringe redesign helped to partially alleviate the issue, the problem was not completely fixed. With the unchanged design, barely any mixture could be deposited before the rest of the mixture got aggregated and rapidly cured. Pressure-cured mixture is too solid to be able to flow, and has

to be removed using water and a tool to chip it out. The issue is alleviated by significantly increasing the outlet diameter and decreasing mixture viscosity, but the latter option is limited because of inability to keep shape upon deposition. The best combination of deposition conditions that could be achieved was deposition at 0.3 bar pressure provided by the fluid dispenser, with the outlet diameter of 7 mm. This way, the samples could be made with a more-or-less macrostructure, with roughly half of the mixture curing inside the syringe and the other half being deposited with varying degrees of success.

The sample printing pattern consisted of four lines, two besides each other with two more placed on top, like in Figure 5.3. The length of the lines was selected to be the same as the length of moulded samples, i.e. 30 mm. Two separate sets of programs were created. The first set is just one program which prints all four lines in one go, and second set is just the first set separated into two separate steps with a delay. This way, part of the samples can be printed without a long delay between the layer deposition, and another part will have a delay between layer deposition. This variation can give information about the impact of printing time on mechanical properties of resultant mixture. Theoretically, having layers deposited with a delay causes them to have different progressions in their curing process, which can introduce inhomogeneity into the material bulk through not allowing polymeric links between the layers to form. Potential decrease in mechanical properties of the samples printed with delay can potentially lead to the conclusion that printing has to be done as fast as possible to ensure good properties. When it comes to the printing projects of large scope, namely habitats, the inevitable printing delays might create issues and hence have to be taken into account.

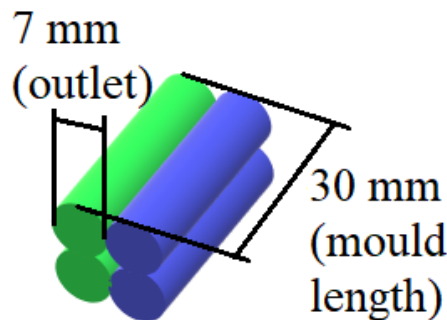


Figure 5.3: **Printing pattern for the 3D-printed samples. Green lines are printed towards from the front, blue are printed away from the front. Top two levels are either deposited immediately or after 30 minutes, to test the mechanical property variance with printing delays.**

During preliminary testing, it was found that overall the deposition of selected paste is inconsistent and it can take several tries to obtain a sample suitable for testing. In order to increase the chance of successful printing, the syringe was being kept closed from the outlet side upon pouring the mixture in and closing it with a fluid dispenser cap. Without such measure taken, most of the mixture liquid could flow away from the outlet, leaving the powder inside with significantly higher regolith to binder ratio than intended. Such solid mixture was not printable. Closing the cap with



closed outlet kept the liquid in using the pressure equilibrium between the ambience and inside of the syringe. In the program itself, feed on delay was not required. When pouring the mixture into syringe, the mixture had low enough viscosity to flow all the way down into the outlet (hence it had to be closed by for example a surface of a plastic cup). Upon closing the syringe with fluid deposition unit connection, bottom of the outlet was effectively the boundary for the mixture, meaning upon pressure application deposition started immediately. Besides, in the end the deposited mixture was flowing over the deposition location anyway, distorting the intended shape, so feed on delay would not have much influence regardless. Retraction height between the lines was kept low (3 mm from the printed sample surface) to help the mixture to be deposited with extra surface tension forces, even though the effect was minimal.

## 5.4. Printing Observations

Overall success of the printing process with proposed mixture is not good, which is reflected in high amount of time spent on figuring out the printing conditions during preliminary testing and the fact that all the propositions from previous section ended up being concepts. Initial plan was for the moulded samples and printed samples to have the same dimensions by having to simply apply some grinding to printed samples to remove deformations caused by material flow. However, after trial-and-error, the minimal acceptable syringe outlet diameter was found out to be 7 mm wide. Lower diameter required high pressure which in turn makes the mixture not printable.

Even with maximized outlet diameter the deposition of the paste was as uniform as desired because of the pressure cure effect, and at times the print had to be attempted multiple times to obtain an acceptable result. With the same printing settings, the amount of material deposited varied between a consistent 7 mm thick line and a series of thick droplets. In the end, because of the material flow, the only difference was the resultant amount of deposited material. Such inconsistency is the reason why printed samples have varying dimensions. The samples with very low thickness (below 4 mm) were discarded, as those had too little material in them and hence were too small to be used in the established three-point-bending test setup.

Mixture curing rapidly under pressure is the reason behind the majority of issues during printing. Because of it the syringe had to be redesigned in the first place, the range of potential regolith to binder ratios decreased, and the printing quality was not satisfactory. PLA material from which the syringes were printed also did not perform under pressure well, so syringes had to be remade several times due to damage. In the current state, the printer model is not compatible with the selected regolith/binder mixture.

## 5.5. Martian conditions

Conditions expected in Martian ambience differ significantly from the ambience on Earth. Settling and hence habitat construction are expected to happen in the lowest layer of Martian atmosphere (Troposphere), hence only this layer is going to be described.

Bottom layer of Martian atmosphere consists mostly of carbon dioxide (95.3%), with some nitrogen (2.7%) and argon (1.6%). The remaining percentage (0.4%) are traces of water vapour, carbon monoxide, oxygen, hydrogen and noble gases [39]. Overall, Martian atmosphere is very thin because gases leak into open space. Because of this continuous leakage, the atmospheric pressure on Mars is very low (6.1 mbar, which is 0.61% of pressure on Earth). This is the reason why water cannot exist in liquid form when exposed to Martian ambience, as it would instantly evaporate. This effect significantly complicates the curing process of geopolymer reaction, as water is an essential component of all the reaction steps. For the dissolution phase of reaction, water is needed for hydrolysis. This step, however is less vulnerable, as dissolution happens fast and can be conducted inside the vessel where mixture preparation occurs. Further steps emit water that is typically trapped inside the material. Low pressure can potentially pull that water from the pores to the atmosphere and cause pores of high size and number, significantly diminishing the mechanical performance. Also, fast release of liquid from the material that has not finished curing significantly restricts the mobility of remaining oligomers and stops the curing prematurely. This has the potential to reduce mechanical properties even further [40].

The temperature at Martian surface is considerably lower than that on Earth, averaging at  $-60^{\circ}\text{C}$ . Near the poles, it can reach as low as  $-125^{\circ}\text{C}$ , and near equator it can rise up to  $20^{\circ}\text{C}$ . Because of thin atmosphere, the variance of temperature is high and can reach  $100^{\circ}\text{C}$  per day in some locations. These conditions, in fact, significantly affect the selection of potential building materials. First of all, materials with curing based upon chemical reaction suffer from reduced temperature significantly, as the reaction rate slows down. Combined with accelerated evaporation rates, reaction-based materials have a very small window to cure. Secondly, large temperature swings drastically impact materials with low thermal stability, inflicting high thermal stresses and reducing mechanical properties over time. Materials selected for Martian mission should have low thermal expansion coefficient to perform well.

The conditions described above are directly related to 3D-printing process on the surface on Mars. However, there are also extra requirements present when investigating the mechanical properties of cured material to ensure good Martian performance as compared to performance on Earth. In addition to low thermal expansion coefficient, the material should have good tensile strength, which is typically not required from building materials. The pressure conditions on Mars are not suitable for humans, and inside the habitat the pressure should be considerably increased up to at least 0.12 bar, at which human can survive with a supply of pure oxygen only. Such pressure is already 20 times higher than the pressure on Mars. Without pure oxygen, this pressure has to be increased even higher. Such pressure difference would induce significant stress on the circumference

of a building (assuming dome-shaped building). Besides the necessity of good tensile properties, impact strength of the material should also be significant, as thin atmosphere offers little protection from meteoroid strikes. Although there is little control over this phenomenon, ability to withstand minor strikes would already improve the success chance of a manned mission. It is worth noting that because of need for radiation protection the expected wall thickness is high (1-2 m), which already offers good impact resistance by itself.

Overall, the conditions on Mars are highly inhospitable for human settling, which is reflected in requirements for an optimal construction material. Adding suitability for 3D-printing in that list makes the selection even more restrictive.

## 5.6. Laboratory Environment Adaptation

In order to simulate Martian conditions in laboratory environment, some planning and preparations were done during the course of the project. Because of difficulties with printing in room conditions, not much effort was spent on performing printing in suboptimal conditions without adjusting the mixture first. Nevertheless, the concept of low temperature and pressure printing chamber was explored during the project, and is described in this section.

3D printer as a whole was not suitable to be placed into the hypothetical vacuum refrigerator, as the various mechanical and electronic parts would be exposed to extreme conditions. Knowing that operating temperatures is quite small (0-40°C), it most likely cannot withstand vacuum as a whole. Hence, the printing area has to be isolated instead. The concept of printing chamber including most necessary items is illustrated in Figure 5.4. The essential components are: temperature control unit, that is responsible for reaching and maintaining desired temperature, pressure control unit, responsible for decreasing the pressure inside the enclosed area, and the enclosed area itself.

### 5.6.1. Temperature Control

The samples that planned to be printed have small dimensions and get deposited on a prepared plate. For the purpose of low temperature printing, it would be sufficient to keep this plate sufficiently cold. A device like a thermal platform, similar to stirring plates used for solution making, was considered for use, however electronics present inside these devices make them dangerous to be operated in a decreased pressure environment. It was decided to investigate a more robust option for temperature control, namely Peltier effect module (Figure 5.5a).

Peltier module consists of two ceramic plates with a set of conductors between them. These conductors consist of two different conductor materials with dissimilar electrochemical potential. This difference makes heated electrons to move to one direction upon heat application, namely to the "hot" ceramic plate, upon the increase of voltage. The opposite of Peltier effect is Seebeck ef-

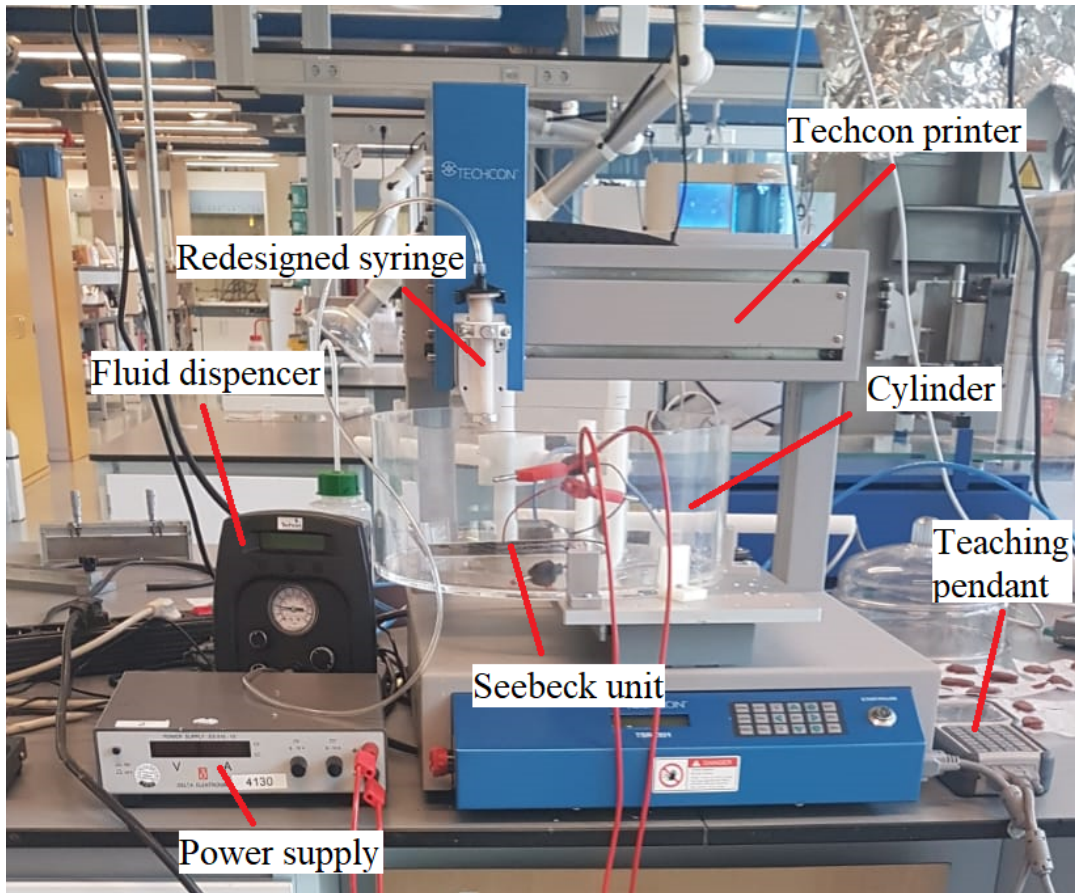


Figure 5.4: Partially assembled 3D-printing setup for simulating Martian conditions. Outside of the picture water temperature control unit is stationed. Some components which are mentioned further in the section are not included (silicon cover, coiled pipe, vacuum pump, drilled holes in the cylindrical chamber).

fect, which generates voltage upon applying temperature difference. The device for Seebeck effect is very similar to Peltier device, and can be used for this application as well because of reversibility of the process. The only cost of using a "wrong" module is efficiency, assuming that specifications allow for operation in desired temperature range. In fact, only Seebeck module was available for the testing during the project, and temperature difference of  $40^{\circ}\text{C}$  was achieved between the plates. This makes it applicable for the purposes of this modification, as achieving  $0^{\circ}\text{C}$  surface temperature can potentially be done just with a cold water heat sink on the hot side of Seebeck module. Looking at Peltier module specifications, they are in general smaller than Seebeck modules and are less resistant to abnormal ambient conditions [41].

In order to maintain the constant cool temperature on the cold plate, it is necessary to have a heat sink which can cool down the hot side of the plate. For this purpose, a coiled pipe can be used through which cold water gets pumped by a water pump unit. Water pump unit simply sets the water to a desired temperature, and pumps it through an enclosed pipe cycle. The coiled pipe design is presented in Figure 5.5b. It is necessary for the pipe to be coiled to ensure high contact area with the Seebeck module. Bent outlets are necessary in order to connect the pipe to the water pumping unit outside the pressurized chamber, which simplifies the design. The pipe should be made out of

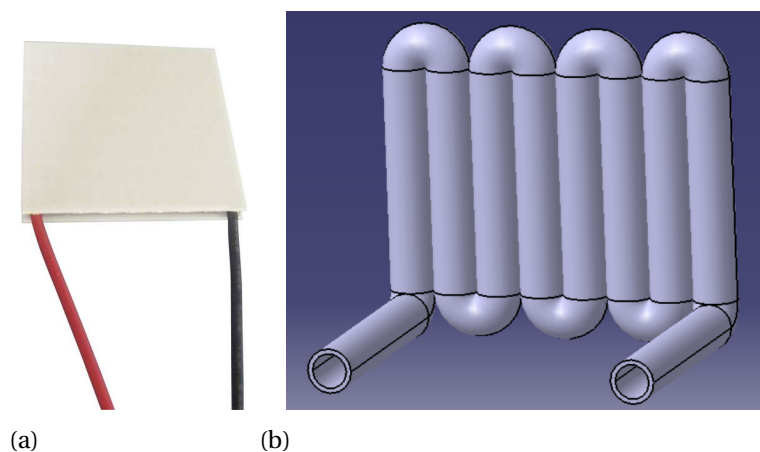


Figure 5.5: **Components related to temperature control inside the printing chamber. a) a Peltier module [6]. b) Coiled pipe design.**

metal, as metals can withstand the low pressure conditions and have high thermal conductivity. In this particular case the outer diameter of the coiled pipe was 15 mm. The pipe should be mounted lowermost part of the enclosed chamber, Seebeck module should be put on top of it in such a way that the hot side is downside and covered with sufficient amount of thermal grease to ensure good thermal conductivity. On the cold side of the module thermal grease has to be applied, so that the deposition plate gets cooled down as efficiently as possible. To ensure the correct temperature setting, a thermocouple wire can be attached to the printing plate. The wire has to be led through a designated hole in the chamber and have sufficient protection from vacuum environment.

### 5.6.2. Pressure Control

In order to control pressure inside the printing chamber, it is necessary to build said printing chamber. Because of the printer structure, it is necessary to have a part of the moving head inside the chamber. Hence, the most convenient way to construct the chamber is to have a solid bottom, where deposition occurs and cooling setup is located, and a flexible cover on top of the solid part, that accommodates for a moving syringe mounting unit (Figure 5.6c). Including more parts of the printer inside the chamber is undesirable, as there is a high chance mechanical parts can be damaged. One of such issues would be dissipation of the heat generated in wires during the printing process, as convection in near-vacuum environment is very limited. The solid part is a thick-walled cylinder, made from a transparent plastic (Figure 5.6a). Cylindrical shape is preferred over cuboid, as less sharp ends leads to less stress concentration points during vacuuming process. Besides, designing a flexible cover with cylindrical shape in mind is considerably easier than with rectangular shape, again for the stress concentration reason.

The cover was planned to be made through moulding process by pouring silicon into the mould shape and curing it in there. Cover design is shown in Figure 5.6b. The cover diameter is slightly smaller than the cylinder chamber outer diameter to ensure good grip during the vacuuming pro-

cess, waves are included to reduce the stress during printhead movements, and the central holes are designed so that the cover can be put over the syringe mounting unit. Rectangular hole tightens around the mounting mechanism, while the circular hole tightens around the syringe. The moulds were 3D-printed using PLA material. Important design considerations when it comes to mould are including enough holes through the top mould half in order to inject uncured liquid silicon material and allow excess air to escape, and including locks on the outer side of the mould so the upper and lower moulds can be locked together, restricting the movement of the moulds with respect to each other during moulding process. An example of the cover mould design can be seen in Figure 5.6d. This design was printed and tested with Elite Double 22 Silicon, but the result was unsatisfactory. The amount of deposition holes was insufficient, and it was not possible to fill whole the mould before an already thick Elite Double 22 silicon mixture began to thicken and cure. As the result, there were multiple tears in a cured product. To improve the chance of success, a larger amount of holes has to be introduced in the mould design, together with looking for a less thick silicon mixture.

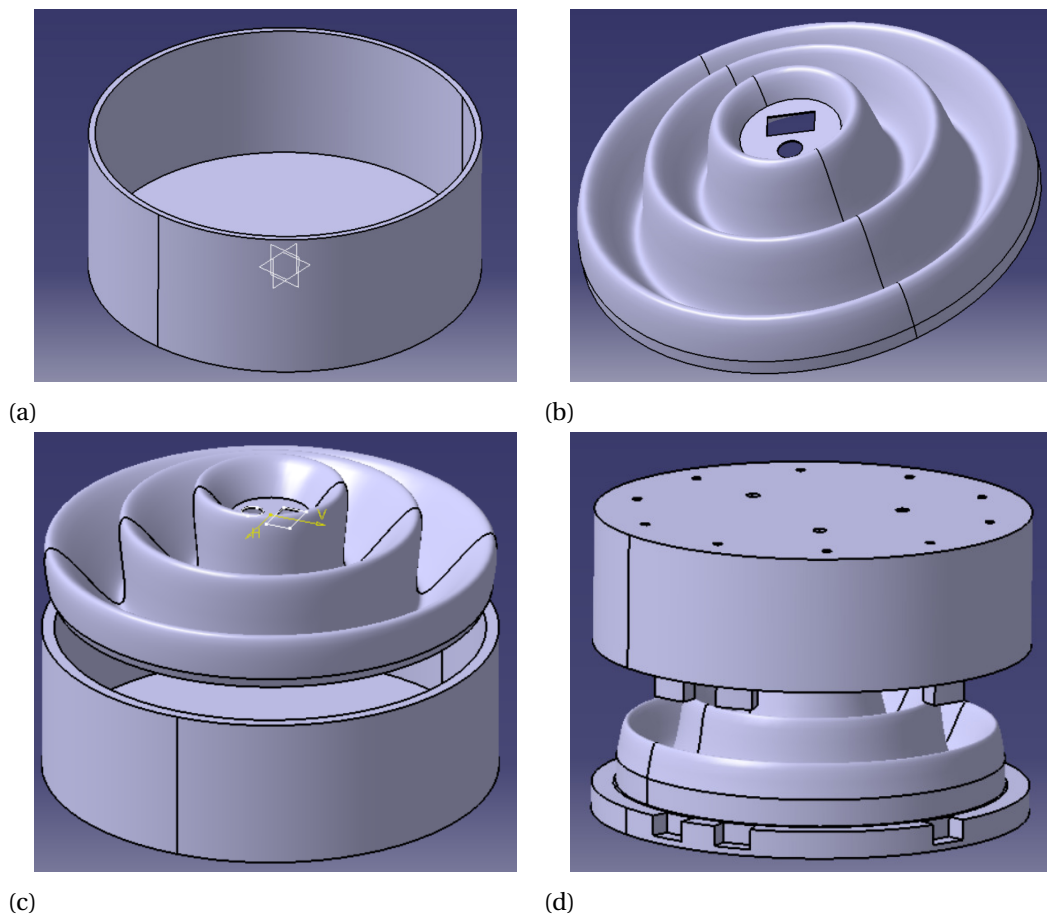


Figure 5.6: **Components composing enclosed space inside the printing chamber for pressure control. a) Transparent solid cylindrical chamber design. b) Silicon cover design. c) Schematic of the cover going on top of the cylindrical chamber. d) Cover mould design.**

To accommodate the rest of appliances needed for Martian condition simulation, the cylindrical chamber part has to be further adapted. A series of wires and pipes have to go through the cylin-

dricial chamber walls. Every such pipe or wire has to have a specially drilled hole, and the hole has to be sealed tight when filled. Otherwise, there is a risk of air leakage, making it impossible to make vacuum. This is the reason why heat sink pipe has outer sides bent downwards (Figure 5.5b) - so that these parts can go through the bottom of the cylindrical chamber and be fixed in that position by sealing. Connecting the pipe to the water cooling unit can be done outside of the cylindrical chamber. With the current set up, the holes that have to be drilled are: 2 for Seebeck unit wires, 1 for thermocouple wire, 2 for the coiled pipe, 1 for the vacuum pump pipe. The confined space can be opened and closed by the means of removing the flexible cover from the cylindrical chamber. To simplify sealing, it is better to drill the holes in the bottom part of the cylindrical chamber, as sealing a flat surface is easier than a curved surface. The cylindrical chamber has to be fixed with hooks and screws to the build plate (Figure 5.4), as a large part of the cylindrical chamber has hang outside of the plate to accommodate for wiring.





# 6

## Results and Discussion

Manufactured samples were used to make a conclusion about the viability of the selected mixture. For that, a series of measurements and observations were performed and recorded. Some important information was already obtained during moulding process through visual and tactile observations, as shown in Section 6.1. Measuring mass of the samples and volume allowed determination of density, and explained in Section 6.1.3. Three-point bending test was used as a primary mechanical test, from which elastic modulus (Section 6.1.4) and ultimate flexural stress (Section 6.1.5) were calculated. Analysis of presented results together with the viability of the findings are present in Section 6.2. Finally, the implications of this analysis to real Martian applications are discussed in Section 6.3.

### 6.1. Results

#### 6.1.1. Mould removal

A stark contrast between different samples already arose when removing them from their moulds. In fact, one of the reasons to remove samples during the curing process and not afterwards was the danger of destroying the sample. This was especially noticeable when curing the samples in the oven at high temperature ( $60^{\circ}\text{C}$ ). In addition to hardening, the sample also expands at temperatures higher than it was during deposition, which was done at room temperature ( $23^{\circ}\text{C}$ ). This made the sample not removable from the mould without forcefully separating it from the walls with a thin object like razor. This, in turn, caused chipping and cracking of a fully dried out regolith mixture, deteriorating mechanical properties. While room temperature and low temperature samples were easier to remove because of no expansion happening, there was still a risk of damage due to fragility. Regardless of these reasons, removal during the curing was necessary to ensure uniform curing from all sized of the sample.

The samples were removed from the mould during the second stage of curing, timing for which was derived during DSC analysis and preliminary testing. During the first reaction stage the mixture

is not yet gelled, meaning it loses shape upon the attempt to remove it. During the second curing stage gelation has already occurred, but softness because of incomplete curing is still present. This allows the sample to be removed with minimal damage to it. High temperature samples ( $60^{\circ}\text{C}$ ) were removed after 40 minutes in oven, room temperature samples ( $23^{\circ}\text{C}$ ) were removed after 120 minutes, and low temperature samples ( $2^{\circ}\text{C}$ ) after 5 hours. At these time frames the samples were soft enough to be removed easily, but cured enough to not be damaged.

Overall, the procedure of adjusting mould removal gave information about the fragility of the samples and confirmed the sample curing properties. The two-stage cure was visually tracked during the removal timing adjustment, and final product was confirmed to be overall not flexible, prone to crumbling and cracking, with varying extent depending upon the curing conditions. The summary of observations regarding the mould removal process is present in Figure 6.1.

When it comes to curing time, temperature is the detrimental factor, while pressure seems to have little to no effect on it. While curing samples at ( $60^{\circ}\text{C}$ ), it was easy to see that total curing time took around 6 hours for all 3 different pressure conditions. The state of sample cure after 6 hours was identical by the end of this time, and the progress was checked every 30 minutes. In comparison, total curing time for room temperature samples took around 30 hours. Total curing time for samples at the lowest temperature, ( $2^{\circ}\text{C}$ ), took 72 hours, which is considerably longer.

As expected, an increase in the size of a sample also increases the total cure time. This was confirmed by looking at the curing time of the printed samples, that overall had higher dimensions than moulded samples and took longer time to fully cure (around 40 hours for the largest printed sample at room conditions). This, together with high temperature dependence, might be a serious issue when it comes to printing object of larger scales, such as buildings.

During the curing process of the printed samples, the deposited mixture was flowing over the paper as no walls were present to restrict the movement. This caused irregularity in dimensions, as it can be seen in Figure 6.2. Because of this irregularity larger samples took longer time to fully cure than smaller ones. No mould was used for printing the samples, hence no observations regarding mould removal could be made.

The fact that printed mixture was spreading over the deposition location can be vital in evaluating the printing viability. While manufacturing through moulding produces samples of fixed dimensions, in the case with additive manufacturing the sample dimensions vary. As explained in Section 5.4, the printing process with limited outlet diameter has an issue with pressure required for mixture deposition. Applied pressure causes the part of the mixture that does not get deposited fast enough to rapidly cure, solidifying it in the process and making it unsuitable for further printing. Roughly same amount of mixture was prepared for each sample print (10-11 g), but mixture amount that was actually deposited for each sample varied. This effect can be seen in Figure 6.2 between images d) and e), where sample d) had less mixture deposited as the second layer that sample e),

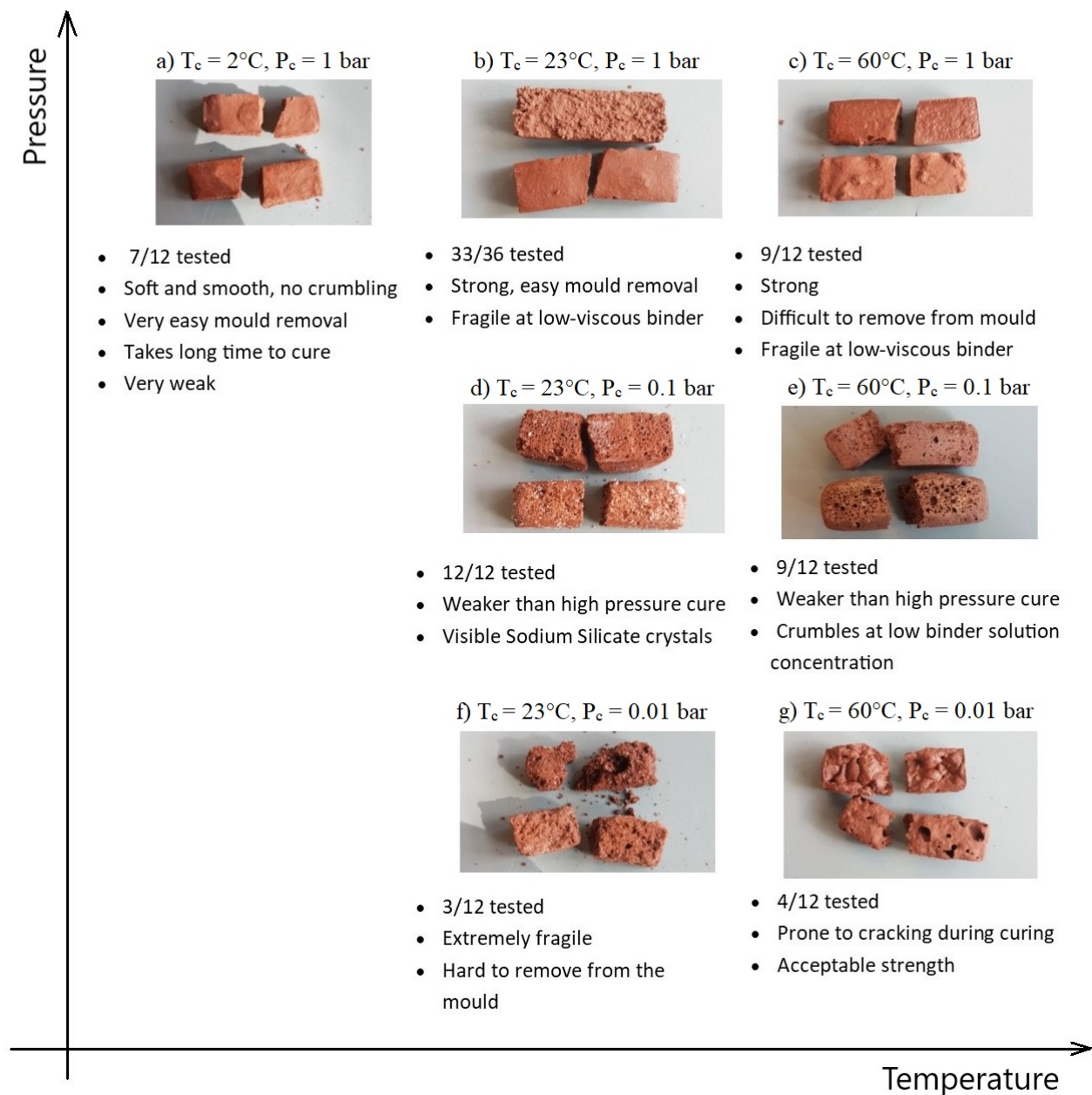


Figure 6.1: Pictures of some of the moulded samples and corresponding observations. Number of tested samples indicates the amount of samples that were robust enough for starting three-point bending test without the sample being broken during the test initiation.

where first and second layer are the same. Between samples a) and c), sample c) has overall larger dimensions than sample a) as more mixture managed to get deposited before mixture solidification. By using large syringe outlet diameter, the paste can be deposited under smaller pressure, but the used diameter of 7 mm could not be increased because of printer functionality restrictions.

As for the differences between printing whole the sample in one go and printing it with a delay,

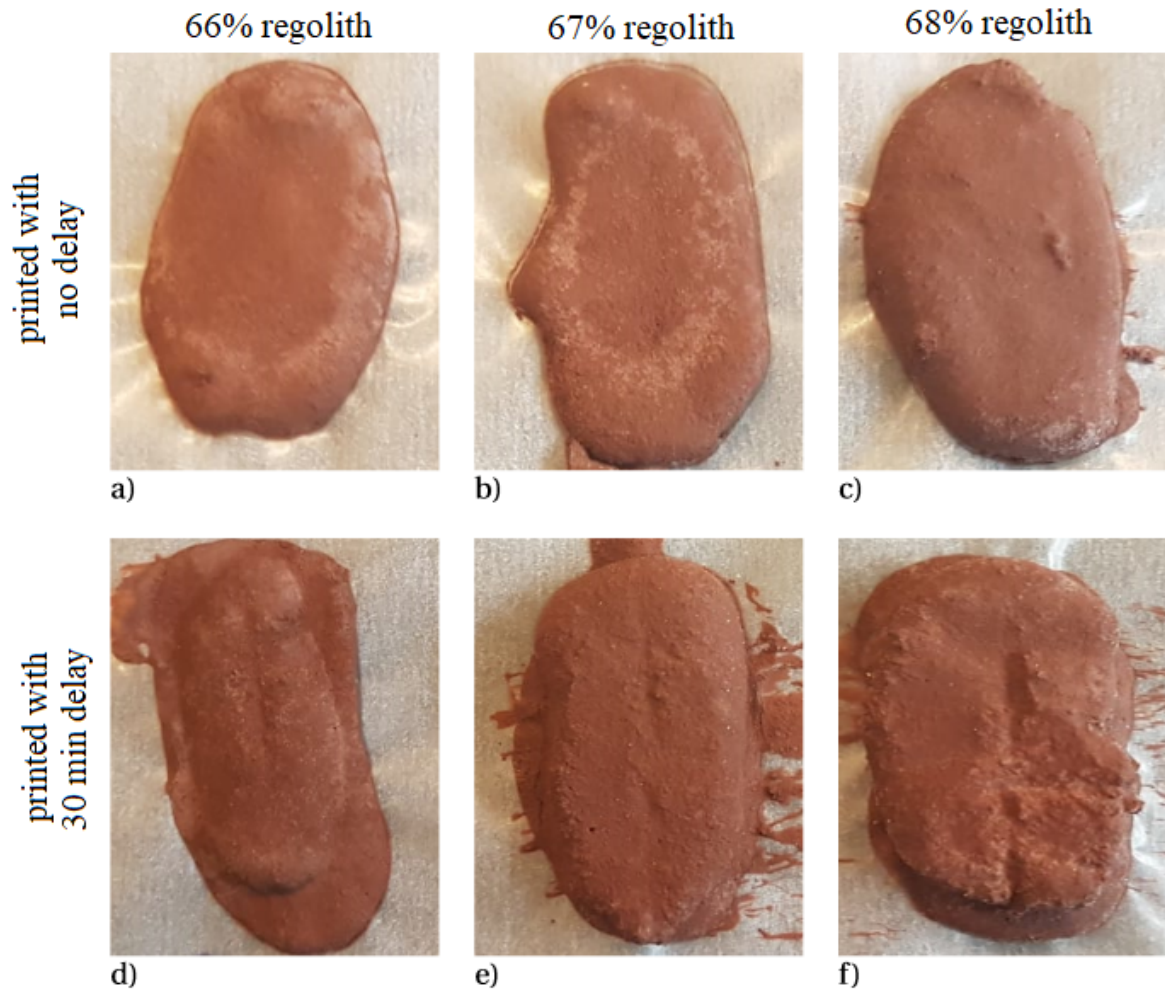


Figure 6.2: Images of printed samples with initial binder concentration of 45%. a) 66% regolith, printed without delay . b) 67% regolith, printed without delay. c) 68% regolith, printed without delay. d) 66% regolith, printed with delay. e) 67% regolith, printed with delay. f) 68% regolith, printed with delay.

visually the difference is clear. Samples without delay (Figure 6.2 a) to c) ) were spread over the deposition location more than their counterparts (Figure 6.2 d) to f) ) and were thinner. Samples with printing delay had a clear border between the layers. This indicates that the curing reaction that partially completed in the first deposited layer progresses far enough that the second deposited layer does not get fully incorporated, and mechanical properties on the border between the layers are likely different than inside the layers. If this phenomenon affects overall mechanical properties negatively, which is likely because of introduced inhomogeneity, it is another argument in favour of increasing syringe outlet diameter when designing 3D-printing equipment.

### 6.1.2. Pore characteristics

Porosity of the samples was directly related to curing pressure of the samples, as it can be seen in Figure 6.1 (a - g). Curing completed at atmospheric pressure 1 bar (Figure 6.1 (a - c)) did not induce any visible porosity in the samples. Samples cured at a tenth of atmospheric pressure 0.1 bar ( d)

and e) ) have small uniform pores through all the sample material. Samples cured at even lower pressure 0.01 bar ( f), g) ) have several large pores instead of a large amount of small ones. Additionally, surfaces of these samples look rugged and irregular.

Significant increase in visible porosity of the samples cured at decreased pressure can be explained by the rapid decrease of the boiling temperature of the mixture as the pressure goes down. Decreased content of moisture in ambience achieved through vacuuming process causes the liquid present in the mixture to rapidly evaporate. Lower the pressure, more rapid evaporation becomes. This can explain the difference between pores in the samples: slightly lowered pressure (0.1 bar) makes boiling slower and less rapid, generating small and uniform bubbles. Very low pressure (0.01 bar, slightly higher than Martian pressure) on the other hand causes the boiling process to be more rapid, making bubbles large and also makes the surface of the samples rugged. This especially can be seen on Figure 6.1 g), where the combination of rapid boiling and fast cure managed to visually fixate the surface irregularity.

The problem with this observation is that the pressure on Mars is 169 times lower than that on Earth, therefore large pores as present on samples cured at 0.01 bar pressure are expected if no precautions are taken. Irregularity of such pores might cause high unpredictability regarding mechanical properties when designing anything from such material.

Printed samples had no visible porosity observed, which is expected. There are pores present of course, but those are induced by trapped water during the curing reaction, and are only observable under strong magnification microscope within the material bulk. Curing at room conditions did not indicate any porosity for moulded samples, so similar effect is expected with printed samples. Freedom of mixture movement during the curing process reduces the chance of visible pores appearing even further, as the vacant space can be filled up quicker with more mobile particles.

### 6.1.3. Density

Measuring density of the samples is different for moulded samples and printed samples because of the manufacturing difference, which in turn resulted in sample dimension difference. During moulding, the mixture was poured into a mould of a fixed volume. In some cases, the curing conditions caused the samples to expand, increasing the volume. This was counteracted by grinding the sample from the top of the mould, until all extra material is removed. This had to be done carefully so cracks or chips do not form in the rest of the sample. All the moulded samples had the same dimensions, which allowed for uniform density calculations as well as mechanical testing. For clarity, density values were divided by the average density of regolith powder that was determined in Chapter 2, yielding relative density with respect to the dry material. The results of relative density calculations are shown in Figure 6.3, where density plots are arranged depending on curing conditions for easier comparison.

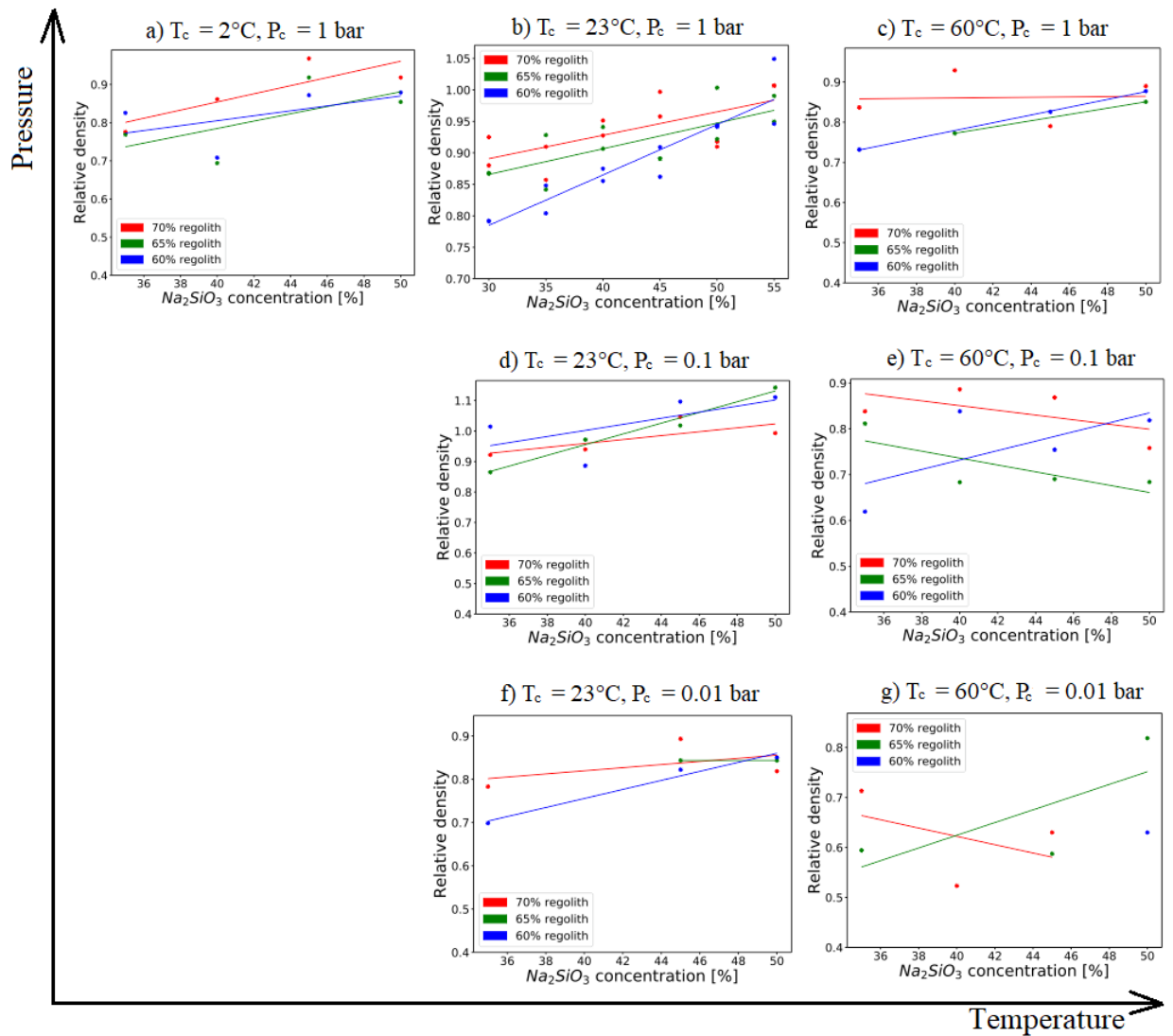


Figure 6.3: Comparison of resultant relative density values for moulded samples

Printed samples on the other hand had varying dimensions because of the non-uniform deposition and material flow during curing process. For these samples, the volume was measured by using the measuring cylinder with water, same as it was done for powder density calculations and is described in Section 2.1. Density were calculated using Equation 2.1. As in the case with moulded samples, relative density with respect to dry material was calculated for clarity purposes. The results of relative density calculations for printed samples are shown in Figure 6.4. Dashed line represents samples that were printed in one go, as indicated in Section 5.3, and solid line represents samples that had a delay between printed layers.

For better overview of the temperature, pressure and printing effects on the density properties, an average value of density was taken from every plot in Figures 6.3 and 6.4, and plotted versus temperature. The summation of all densities for a certain set of conditions was divided by the number of densities to determine an average value. Curves fitting the same pressure values were added for

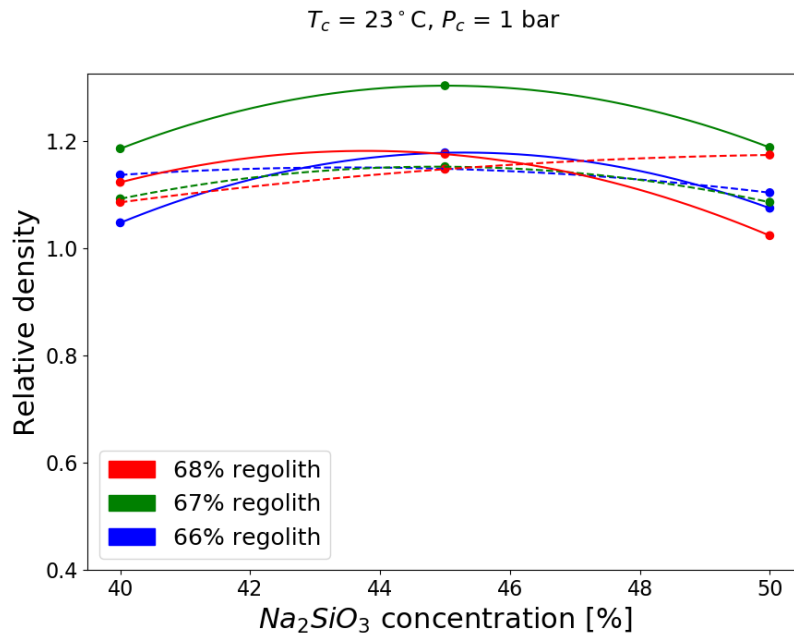


Figure 6.4: **Relative density results from the 3D-printed samples. Dashed lines indicate sample printed in one go, solid lines indicate sample with 30 min delay between deposition.**

clarity. The resultant plot can be seen on Figure 6.5. As printing was done only for one set of conditions, it is represented by two data points. The average values from moulded samples cured at room temperature were restricted to the same binder solution concentration values as used for non-room temperature ones after the elimination process, as samples made with those binder concentration solutions had insufficient mechanical properties to be considered.

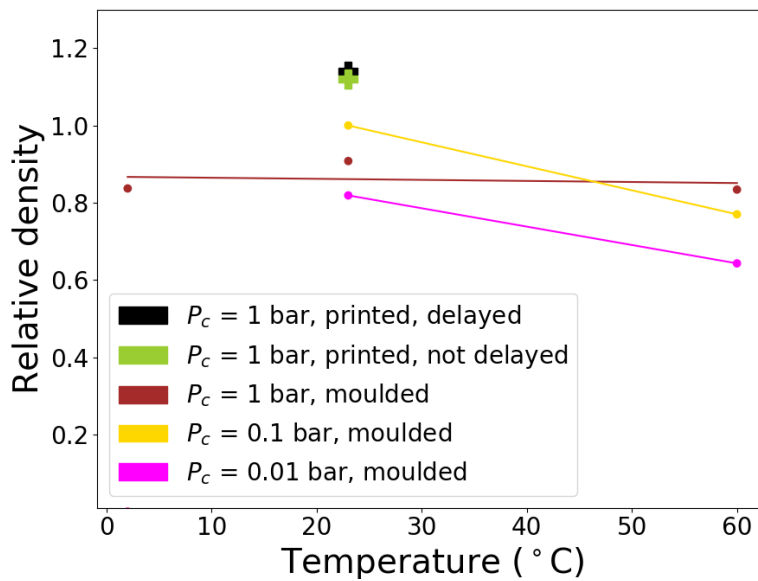


Figure 6.5: **Average relative density across all the samples for certain temperature and pressure conditions**

Average relative density difference between 23°C and 60°C samples is 0.1-0.2. This can be explained by reduced amount of trapped water in the pores inside the material. Higher temperature forces evaporation to occur faster and improves overall molecule mobility, so during the cure process, when mobility of the oligomers is still present, more residual water molecules are able to escape the material bulk and evaporate, as compared to lower temperatures. This observation is also supported by tactile senses, as samples cured at high temperature felt very dry inside the bulk, as compared to room temperature cured samples and especially low temperature ones, which felt almost entirely wet. These observations were made after mechanical testing of the samples, hence after complete curing. At the same time, the density value for samples cured at 2°C temperature is lower by 0.1 than for those cured at room temperature, as it can be seen at the 1 bar pressure points in Figure 6.5. Low temperature means lower mobility of oligomers, which results in less polymeric links and less efficient packing, as despite open spaces oligomers do not have enough kinetic energy to relocate.

For better information about pressure effect on density, tests at more conditions would be useful for the results to be more conclusive. At high temperature, clearly lowering the pressure decreases the density as water present in the mixture is forced to evaporate into near-vacuum ambience (Figure 6.5). This creates pores, which become permanent in the bulk of material because of fast curing times. These pores are visible with naked eye in Figure 6.1. However, as data points related to room temperature conditions show (Figure 6.5), such dependency may not be the case for other temperatures. While 0.01 bar pressure samples still show the lowest density, samples cured at 0.1 bar have clearly highest average relative density (Figure 6.5). Potentially, this could be explained by the balance of reaction rate and vacuum-induced boiling rate. The samples cured at 0.1 bar pressure in room temperature have very small pores (around 0.1-0.5 mm), while 0.01 bar pressure samples have large ones (1 mm). Perhaps when the reaction rate is slow enough (in lower temperatures), there is enough time for the curing oligomers to move and fill the space freed up by boiling process. This reduces water amount in the samples and also reduces amount of pores. At lower pressure ( $P_c = 0.01$  bar) however, the pores are simply too large to be easily filled by curing material, as mobility of oligomers is not unlimited. To further test this claim however, more tests have to be done the wider range of temperatures and pressures.

On average, it seems that lowering the amount of regolith decreases density of the samples. This can be easily explained by increased water content, as less regolith means higher binder solution amount in the mixture. Overall higher amount of water means that more sample mass can be lost to the ambience in the form of water, decreasing the density. Same reasoning can be applied to the Sodium Silicate concentration within the binder solution, where lower concentration means higher water content that is free to be evaporated.

Printed samples clearly have higher density than that of moulded samples, being higher by 0.1 comparing to the highest average relative density for moulded samples (at 23°C and 0.1 bar), and higher by 0.2 comparint to samples moulded in the same conditions. During the printing, the mix-



ture was free to flow on the surface of sheet where it was deposited, as supported by the visual inspection in Figure 6.2. Inside the mould, there was less space available for mixture mobility. Hence, after the printing, the mixture had more freedom to rearrange into a more compact and efficient packing, increasing packing density considerably. This mobility was combined with higher surface area for water evaporation. Because of relatively low curing temperature (room conditions), density increased as water was evaporating and allowing oligomers to fill the space. With delayed second layer printing, there was even more opportunity for water to evaporate as essentially an extra layer of water was gone before the second deposition, making density even higher.

#### 6.1.4. Elastic Modulus

Elastic modulus is defined as a ratio between applied stress and sample strain. In the case of three-point bending test, elastic modulus can be determined by taking a linear portion of force-displacement curve, which is the direct result of such test. Figure 6.6 indicates such part of the curve. The force values in the beginning and end of this part of the curve have to be converted into stress using three-point bending formula:

$$\sigma = \frac{3Fl_s}{2wt^2}, \quad (6.1)$$

where  $F$  is the force value (either  $F_h$  or  $F_l$  for elastic modulus calculation),  $l_s$  is the testing bench span,  $w$  is the width of the sample, and  $t$  is the thickness of the sample. For moulded samples,  $w = 10$  mm and  $t = 5$  mm. For all tests,  $l_s = 20$  mm. For printed samples, the dimensions of each sample were measured using a digital caliper, after grinding the samples such that cross-sections had relatively rectangular shape within the span length. The three-point bending test setup with the noted parameters indicated is shown in Figure 6.7.

As next calculation step, the difference of resultant stress values is divided by the strain difference in dimensionless form:

$$E = \frac{\sigma_h - \sigma_l}{e_h - e_l}, \quad (6.2)$$

where  $\sigma_h$  is the stress value derived from the upper part of the force-displacement curve,  $\sigma_l$  is stress derived from lower part of the force-displacement curve,  $e_h$  is strain corresponding to upper part of the curve, and  $e_l$  is strain from lower part of the curve. As the machine measurements were taken as displacement in millimeters, displacement has to be converted to dimensionless strain as:

$$e = \frac{d}{t}, \quad (6.3)$$

where  $e$  is strain,  $d$  is displacement, and  $t$  is sample thickness.

The resultant values of elastic modulus for moulded samples are shown in Figure 6.8. It should

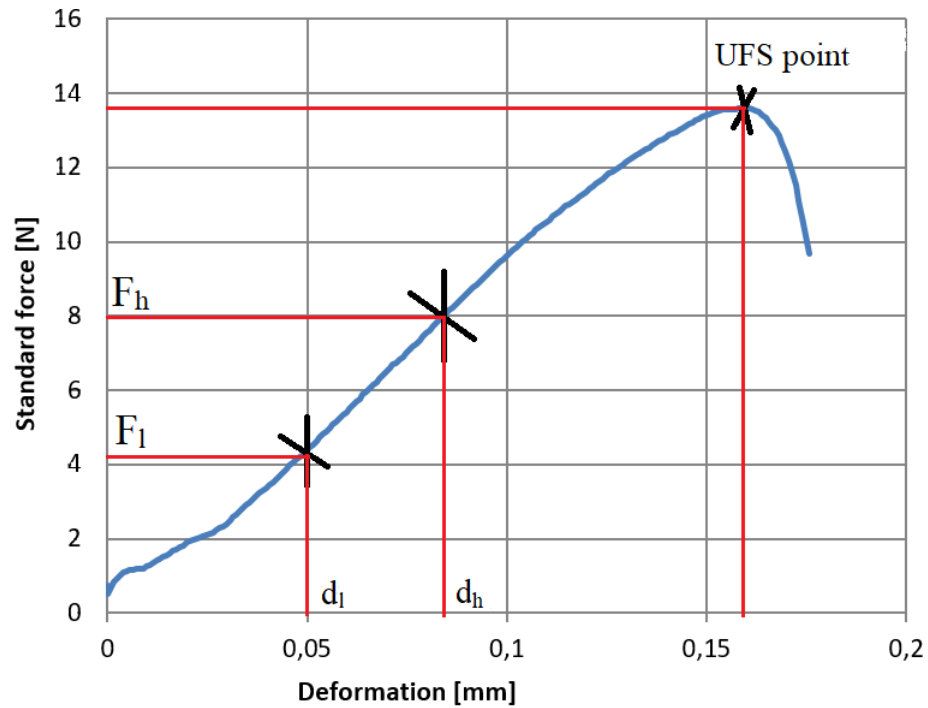


Figure 6.6: Force-displacement curve as the result of testing one specimen in three-point bending test setup. A straight part of the curve is selected for elastic modulus calculations, with respective force and displacement values. Force is converted into stress, and displacement is converted into dimensionless value using sample thickness.

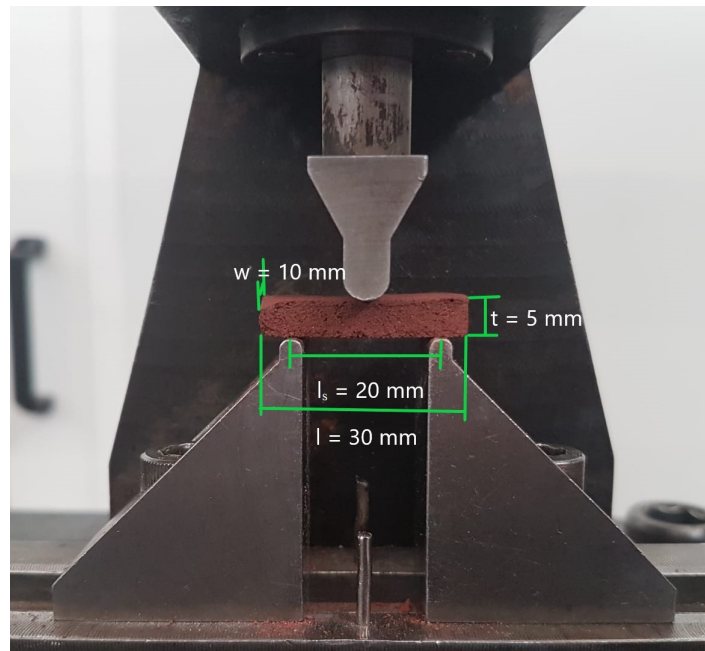


Figure 6.7: Three-point bending test setup with one of the moulded samples.

be noted that some of the plots have a small amount of points. As indicated in Figure 6.1, samples cured at certain conditions were extremely fragile and broke either during mould removal or upon pre-loading part of three-point bending test. Pre-loading force was extremely small (0.5 N), hence those sample can be considered as failed samples. Such failure renders the curing conditions unde-

sirable, as the samples produced are unreliable.

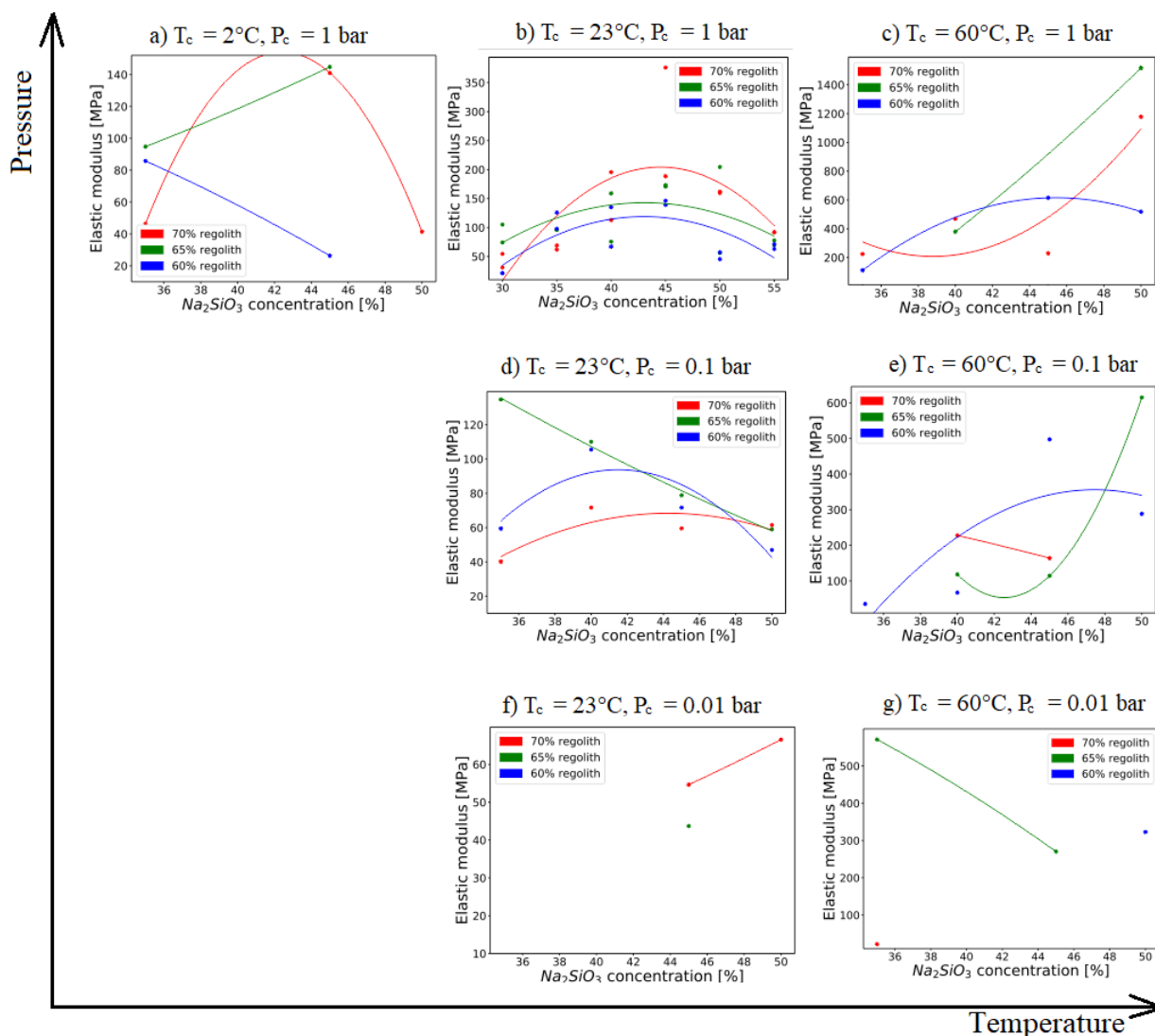


Figure 6.8: Comparison of resultant elastic modulus values for moulded samples

Results of elastic modulus calculations for printed samples are shown in Figure 6.9. As before, dashed line represents samples printed in one go, and solid line refers to samples printed with delay between layers.

Average values of elastic modulus for each manufacturing/curing condition are plotted versus temperature in Figure 6.10, with pressure condition being plotted as a fitting line for easier comparison. As it can be seen, temperature clearly causes the elastic modulus to rise. The difference in elastic modulus for 1 bar pressure between low and room temperature is not large (20 MPa), while the difference between room temperature and high temperature for all pressures is very large, ranging from doubling for 0.1 bar pressure to quadrupling for 1 bar pressure. High temperature increases the mobility of the oligomers, allowing them to interlink into polymers more reliably. This

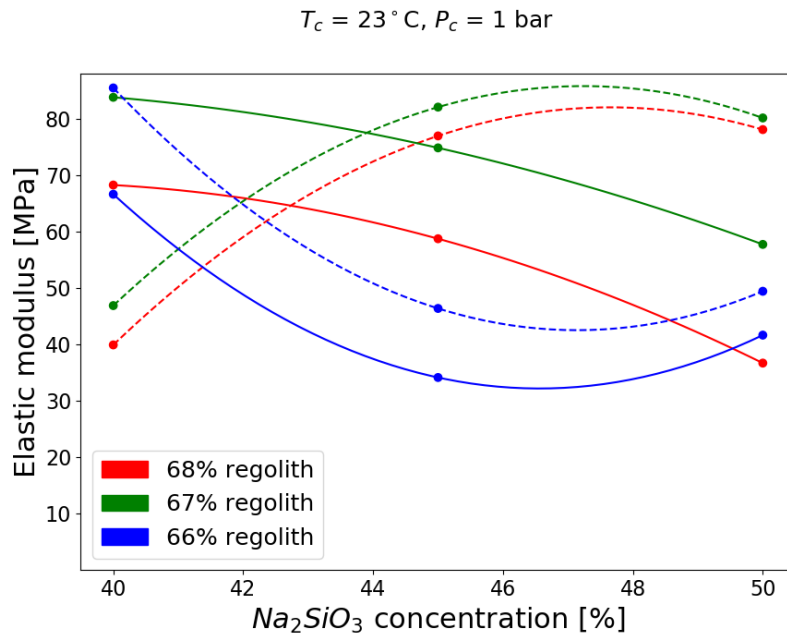


Figure 6.9: Elastic modulus results from the 3D-printed samples. Dashed lines indicate sample printed in one go, solid lines indicate sample with delay.

causes the stiffness to rise, as an interlinked polymer is considerably less mobile than a collection of oligomers that can slide along each other. Also, higher temperatures cause more water to be evaporated, and water creates a liquid medium where oligomers can move more freely as compared to dry medium, which also contributes to increase in stiffness.

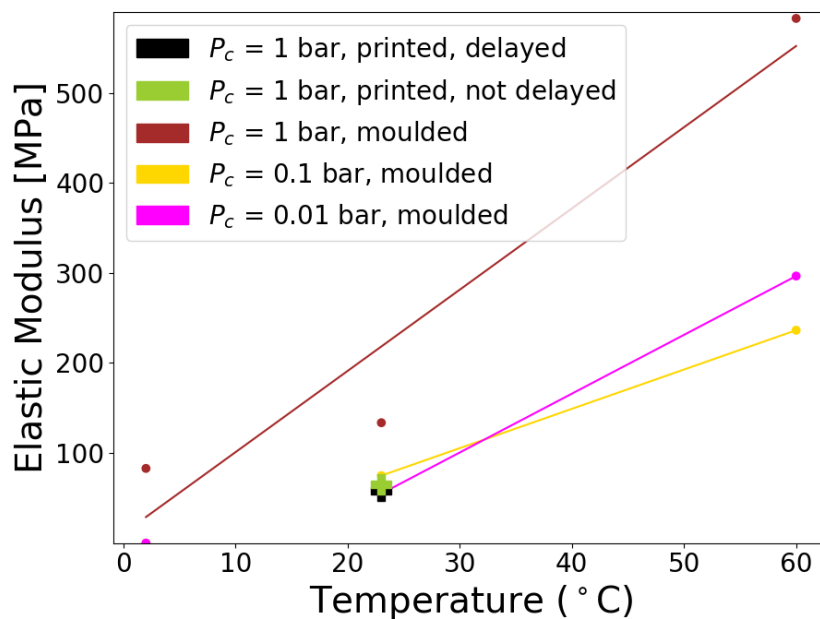


Figure 6.10: Average elastic modulus across all the samples for certain temperature and pressure conditions

When it comes to pressure, elastic modulus seems to decrease with the drop of pressure (Figure 6.10). Between 1 bar pressure conditions and lower pressures, the difference is double at 60°C. Similar to the reasoning behind temperature behaviour, presence of water during the curing allows for better interlinking into large polymeric chains, increasing elastic modulus. As the pressure is decreased, water evaporates and restricts mobility of oligomers during the curing process, halting polymerization. Between 0.1 bar and 0.01 bar, nearly all the water evaporates sufficiently fast with the only difference being the size of pores. This might explain the similar elastic modulus values, as the window for polymerization is reduced in similar amount of time for both these pressures. As smaller amount of polymeric chains allows oligomers to move along each other during stress application, the elastic modulus drops.

Mixture composition effect on the elastic modulus is difficult to analyse from the obtained data, as all the plots except room conditions have small amount of data points without much pattern present. However, looking at room condition cure plot, it can be seen that the peaks of fitted elastic modulus curves for all regolith ratios are around 45% binder concentration. Most likely explanation for this peak is having a closest to optimal ratio of Si/Al, increasing the amount of polymeric links and increasing elastic modulus. Solution concentration of 50% and above introduces too much silicon in the system, causing unreacted areas to appear and decrease elastic modulus. Water content is also an important parameter, as high water content provides a movement medium for the borders between unreacted oligomers. This is illustrated by samples with lower regolith content having lower elastic modulus.

Looking at the average values in Figure 6.10, printing clearly reduces elastic modulus of the material to the levels of low-pressure cure at room temperature (58 MPa for delayed samples and 65 MPa for non-delayed on average as compared to 134 MPa for moulded samples). During moulding, mobility of the mixture is very limited, and deposition is done very fast by pouring the material. Printing introduces a delay while the syringe is working (programmed printing duration is 8 seconds), and the mixture spreads over deposition location afterwards. This induces the variations in reaction progression across different bulk locations. While parts of the mixture is flowing and rearranging to achieve optimal packing, some other parts are already settled and reaction is progressed further. Between the particles from locations with different reaction progress, less oligomers can interlink, hence reducing the amount of polymeric links and decreasing elastic modulus. The stiffness of samples with delayed layer deposition is higher than on those printed in one go, as more water manages to evaporate from the sample bulk. This restricts the mobility of oligomers during stress application.

### 6.1.5. Ultimate Flexural Stress

Flexural stress is a direct measurement of mechanical robustness of the material when it comes to actual application. It can be obtained from the three-point bending test data, and is calculated by Equation 6.1. It incorporates both tensile and compressive stress resistance. Normally for the

structural purposes concrete is evaluated only in compressive stress properties. However, for space applications pressure inside the building is expected to be present, and pressure differential load is of tensile nature.

For the purpose of result evaluation, the force at a breaking was taken for the ultimate flexural stress calculation. The point of maximum stress is indicated in Figure 6.6. Point of maximum stress is taken instead of yield point because the material is concrete, which has a very small yield range unlike for example metals. The resultant ultimate flexural stress values for each of the moulded samples are plotted in Figure 6.11. Like in the case with elastic modulus plots, a large amount of points are missing because of insufficient robustness of the samples, which resulted in the test not being executed at all.

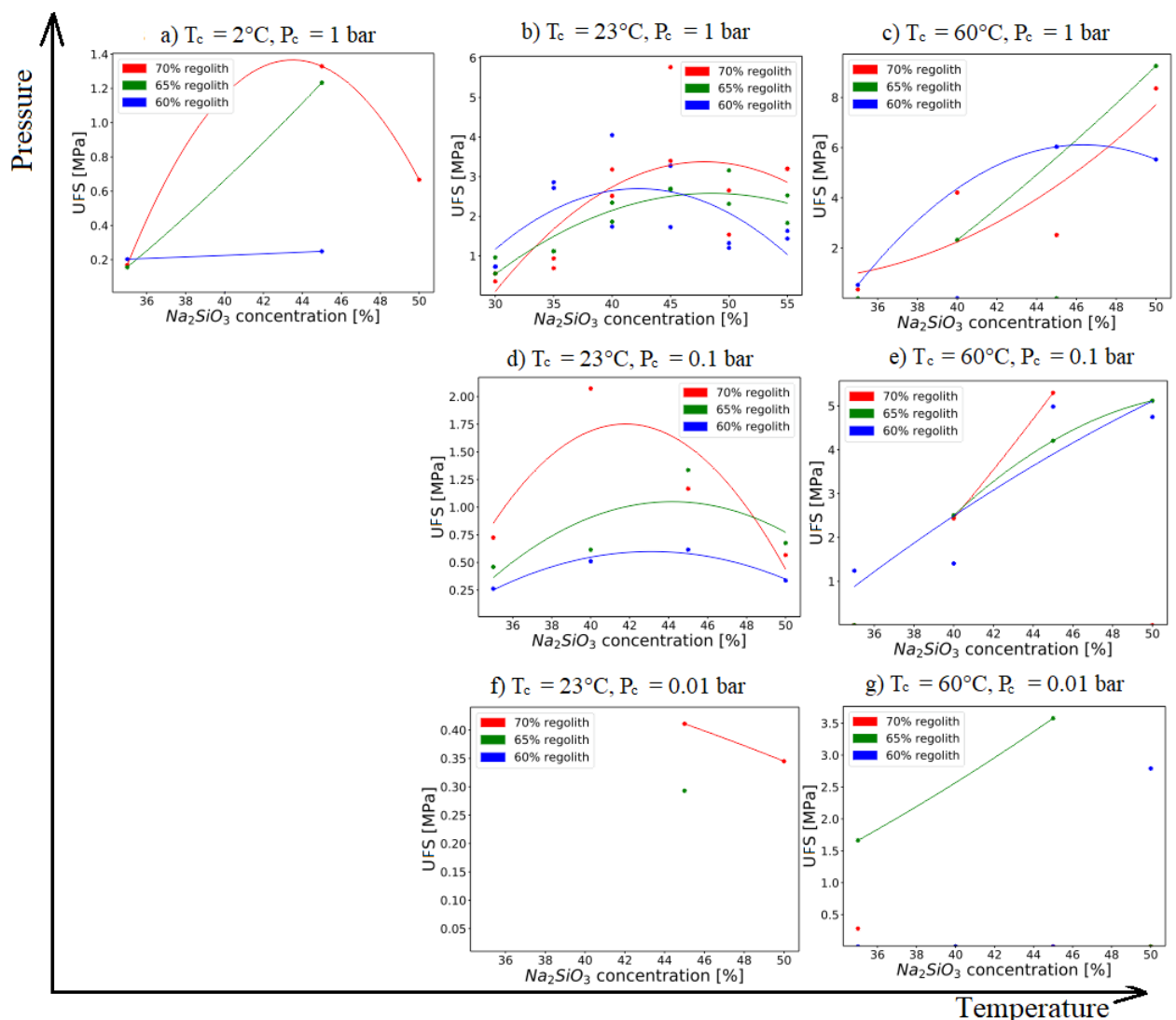


Figure 6.11: Comparison of resultant ultimate flexural strength values for moulded samples

Ultimate flexural stress endured by printed samples is plotted in Figure 6.12. As before, dashed

line stands for samples printed with delay, while solid line stands for samples printed in one go.

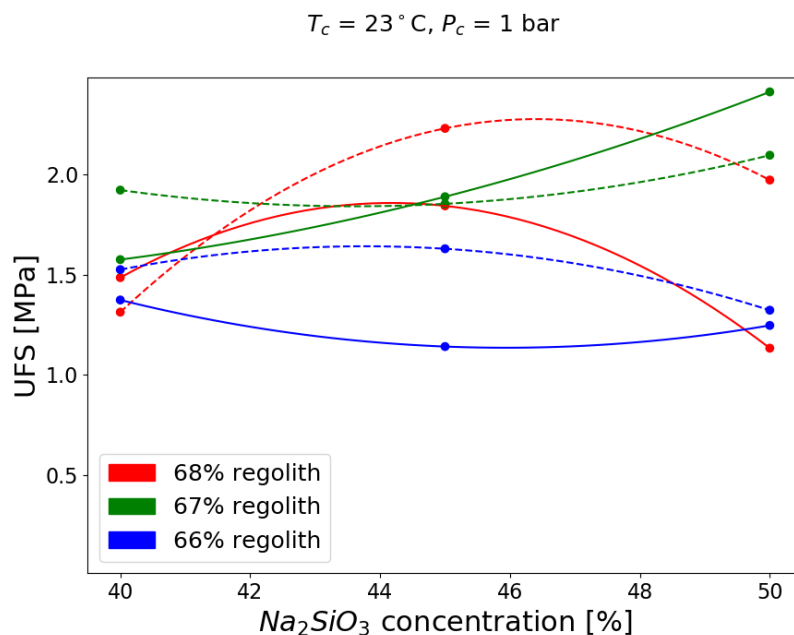


Figure 6.12: **Ultimate flexural strength results from the 3D-printed samples. Dashed lines indicate sample printed in one go, solid lines indicate sample with delay.**

For easier comparison, the average values of UFS for printed and moulded samples at each conditions were plotted versus temperature with fitted lines representing each pressure in Figure 6.13. Printed samples are represented by single crosses as curing was done only at room condition set for samples with and without delay.

Clearly, curing temperature increase directly increases the maximum flexural stress that sample can endure. High temperature allows for higher oligomer mobility and reaction rate, which increases the amount of polymeric links and hence makes the material stronger. The difference in UFS values between temperature steps at each pressure ranged from 83% increase (like between  $23^\circ\text{C}$  and  $60^\circ\text{C}$  at 1 bar pressure), to 425% increase (like between  $23^\circ\text{C}$  and  $60^\circ\text{C}$  at 0.01 bar pressure). This is in accordance with what was observed for elastic modulus (Figure 6.10). Faster water evaporation is also an effect of high temperature. Water emitted during the curing reaction in high temperature ambience is removed from the pores through faster evaporation, however vacant space can be filled by the material assuming it is in the process of reacting and is mobile enough, which high temperature allows. This decreases the volume of non-functional space in the material bulk (pores become filled), and this increases the overall strength.

Decrease in pressure induces rapid water evaporation. This generates pores, which are larger for lower pressure values, and destroys reaction medium for link formation. The formation of large pores decreases the effective volume of material bulk, as pores and unreacted particles do not contribute much when it comes to mechanical properties. Decrease in elastic modulus supports this

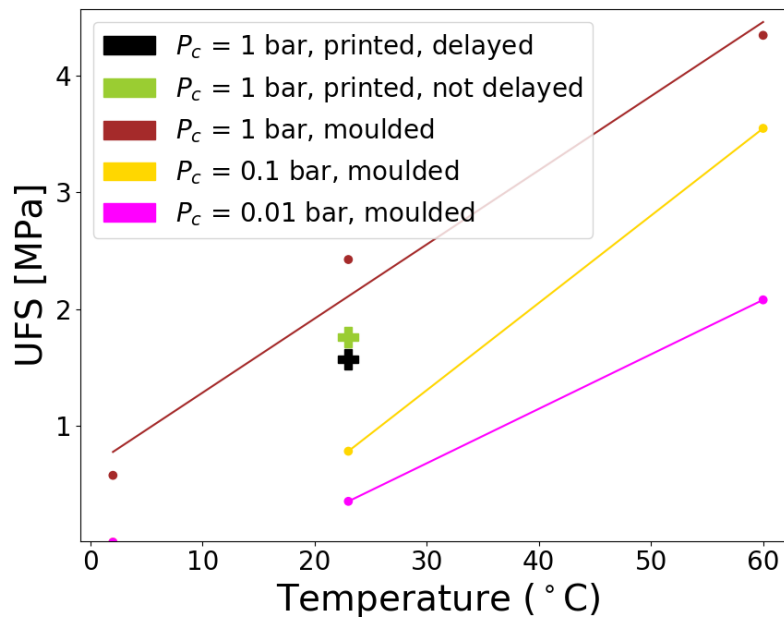


Figure 6.13: Average UFS across all the samples for certain temperature and pressure conditions

observation as well (Figure 6.10).

Like in the case with elastic modulus, the plots outside of room condition curing are hardly conclusive regarding the effect of mixture composition. From the room condition plot (Figure 6.11 (b)) however, it can be seen that again at 45-50% binder solution concentration, UFS reaches the peak values of around 2-4 MPa, with an outlier which achieved nearly 6 MPa UFS at 45% binder concentration and 70% regolith composition. High regolith content also seems to increase the amount of stress that sample can endure. As mentioned earlier, it seems that at binder solution concentration of 45% a ratio of equilibrium between aluminum and silicon is achieved, which peaks the amount of reacted oligomers and yields the highest achieved mechanical properties. Higher amount of silicon shifts this balance away. Low amount of water increases the volume of material that is functional, as soon as there is enough water to allow curing reaction to take place. Considering the mixture compositions for this test were determined in such a way that there is enough binder to wet all the powder, the amount of water should initially be sufficient in all cases.

When it comes to printed samples, the flexural stress behaviour is similar to elastic modulus behaviour. Average highest achieved flexural stress of printed samples is 70% of the value for moulded samples at room conditions. The lack of boundaries around the deposited mixture allow the paste to flow in different directions, changing the reaction progression extent across the material bulk. This reduces the amount of polymeric links formed, as the curing material is not as homogeneous as moulded sample. Delay between printing the layers makes the bulk even less homogeneous, decreasing flexural strength. On the border between printed layers this difference is especially large.



## 6.2. Discussion of the Results

Looking at the result as a whole, the proposed binder/regolith geopolymer mixture looks decent, especially considering the flexibility of binder composition that was not explored in the scope of this project. A large issue arises when considering the fact that for space application ability to cure well in low pressure and temperature conditions is crucial. From this point of view, the mixture is not suitable for space application. An overview of explored curing conditions and their effect on the resultant material properties is shown in Table 6.1.

Table 6.1: **Viability of tested samples with respect to cure conditions. Green cells indicate good conditions, yellow indicate conditions that produce somewhat useful material, red indicate poor cure conditions.**

| $P_c$<br>[ bar] | $T_c$<br>[°C] | 2  | 23   | 60   |
|-----------------|---------------|--|--|--|
| 1               |               | <ul style="list-style-type: none"> <li>◦ very weak mechanical properties</li> <li>◦ low robustness</li> <li>◦ no porosity</li> <li>◦ long cure time</li> </ul> | <ul style="list-style-type: none"> <li>◦ good mechanical properties</li> <li>◦ good robustness (most compositions)</li> <li>◦ no porosity</li> <li>◦ medium cure time</li> </ul> | <ul style="list-style-type: none"> <li>◦ good mechanical properties</li> <li>◦ decent robustness (most compositions)</li> <li>◦ no porosity</li> <li>◦ fast cure time</li> </ul>     |
| 0.1             |               | N/A  | <ul style="list-style-type: none"> <li>◦ poor mechanical properties</li> <li>◦ good robustness</li> <li>◦ some porosity</li> <li>◦ medium cure time</li> </ul>                   | <ul style="list-style-type: none"> <li>◦ decent mechanical properties</li> <li>◦ decent robustness (most compositions)</li> <li>◦ high porosity</li> <li>◦ fast cure time</li> </ul> |
| 0.01            |               | N/A  | <ul style="list-style-type: none"> <li>◦ poor mechanical properties</li> <li>◦ unacceptable robustness</li> <li>◦ high porosity</li> <li>◦ medium cure time</li> </ul>           | <ul style="list-style-type: none"> <li>◦ decent mechanical properties</li> <li>◦ low robustness</li> <li>◦ high porosity</li> <li>◦ fast cure time</li> </ul>                        |

The role of water in the curing process of geopolymer mixture is crucial. It is required for the hydrolysis of powder particles, and then it gets emitted during polymerisation process and provides the medium for polymerisation to occur. Decreased pressure causes water to rapidly evaporate and leave pores in material bulk, which ends curing reaction prematurely and introduces inconsistency in the material bulk. Increase in temperature can help bypass the rapid loss of water by speeding up the reaction. However, a combination of low temperature and pressure yields material that is hardly useful for construction purposes. In this project, the experiments with samples cured at low temperature (2°C together with reduced pressure (0.1 and 0.01 bar) were not able to be conducted, but looking at the pattern formed by conducted experiments the expected results are not good either.

The ratio between aluminum and silicon in the mixture also affects the resultant mechanical

properties, although to a lesser extent in this particular set of experiments. As mentioned in Section 3.5, staying within an optimal range of this ratio (1.65-1.9) allows most of the material to react into large polymeric chains. Suboptimal ratio introduces unreacted pockets within the material bulk, increasing inhomogeneity and decreasing mechanical properties. In this report, optimal silicon to aluminum ratio seemed to be achieved at 45% binder concentration mixed with regolith at 70% regolith to binder ratio. Modifying the binder mixture by for example adding a hydroxide might shift the balance as well, for better or for worse. It is important to track this ratio in order to optimise the mixture properties and ensure the best possible performance.

In the current binder composition iteration, a large amount of binder with respect to regolith is required to incorporate all of the powder into a mixture. Lowest ratio of binder to regolith that was achieved is 30/70, and the resultant mixture was very viscous and inconsistent at times. Such ratio is very high when it comes to transportation costs of the binder from Earth to Mars, especially considering that literature values indicated 2% binder amount in the mixture being sufficient. While potentially required elements can be extracted from various sources on Mars and processed into binder components, technologically such idea is far from being possible. From this point of view, it is required to modify the binder composition so it is required in a considerably lesser quantity. Otherwise, considering that buildings are going to be constructed from this mixture in real life application, the payload mass to be transported is too high together with all the supporting equipment to be viable.

When it comes to printing, a lot of phenomena come into picture that complicate the process. It was found out that the mixture becomes compressed and rapidly reacts under pressure during deposition, which makes it unprintable. This was expected for such a reaction, as oligomers are forced to reallocate into the most compact structure possible, reacting with each other. This effect caused the mixture to be deposited unevenly, skewing the results and complicating printing process. Delays between the layers deposited by printer also affect the resultant properties in a negative way, as the material bulk becomes inhomogeneous. Viscosity of the mixture is highly dependant upon the regolith content, and even a difference of 2% makes a significant difference when it comes to printing. Limited outlet diameter of the syringe that could be achieved during the project (7 mm) also limited the ratios of regolith to binder that could be used to obtain data. As expected, changing manufacturing method from simple moulding to 3D-printing is a considerably more complicated process which introduces multiple issues that have to be solved during mission design.

### **6.3. Application to Mars**

Overall mechanical testing results for sodium silicate cured regolith powder do not look promising when applied to Martian environment. In current iteration, the mechanical properties of the mixture after being cured in either low pressure or low temperature are unsatisfactory, and it is safe to assume that combining low temperature and pressure to simulate Martian conditions would make

the situation even worse. Low pressure has to be counterbalanced by significantly increasing the reaction rate, which is done by either high temperature or modification of the mixture. Low temperature has to be counterbalanced by helping the particles to arrange into efficient packing, which is done by either increasing pressure or, again, modification of the mixture.

When looking at potential solutions in the context of Martian application, increase in temperature can be achieved by choosing a landing location where highest temperatures are achieved (around 20°C). This temperature is achieved in equatorial regions during the Martian midday in summer. However, curing process takes well over 24 hours, and day on Mars lasts 24 hours 37 minutes, meaning lowest temperatures as expected during the night also will be present over the course of curing. Hence, additional heating mechanism is required. This can be done in the form of lamps radiating heat, or creating an enclosed dome which can also provide pressure increase. The former option consumes a large amount of energy, but otherwise requires little equipment to be used. The latter option requires a dome that is larger than a planned building, which required a very large amount of resources to be brought/made. Heating lamp or even a sintering laser can be viable solutions to this problem. The dome, assuming it would be used for printing purposes only, seems like too large of an investment to be justified. Overall, in order to reduce the amount of resources during 3D-printing on Mars, the binder mixture has to be modified with at least adding a hydroxide into the mixture, as suggested in the literature.

When it comes to printer design, a crucial parameter that has to be maximized is the outlet nozzle diameter. Large diameter allows for thicker paste, which reduces the amount of binder required and decreases the flow, allows for lower deposition pressure, which is needed to keep the paste uncured, and allows for layers of higher thickness to be deposited, which increases mechanical properties of the complete structure. It is worth noting that the delays between layer deposition are inevitable because the structure to be printed is of a size of a building, making printing process considerably longer than printing small laboratory samples. The printer for space mission is expected to be designed from scratch, so incorporating as large nozzle diameter as possible should not create issues. A nozzle cap can also be added to the printer structure, keeping the paste inside the syringe when printing does not happen and opening up during the printing process.





## Conclusion

In this project, a geopolymeric mixture with the implementation of Martian regolith was investigated as a potential constructing material for a Martian base. The goal of this project was to study the effect of reduced temperature and pressure on the physical and mechanical properties of cured geopolymeric material. The other objective was to look at the properties of the geopolymeric mixture with respect to 3D-printing, as this is the manufacturing method that looks very promising when it comes to space construction without human interference. The results of this study showed that the properties of the mixture can be improved by either increasing temperature, hence speeding up the reaction, or increasing pressure, thus slowing down the water boiling out. Other improvements to the mixture include increasing the alkalinity of the solution, which significantly speeds up the reaction, and is typically done by adding a strong hydroxide to the binder solution. Testing conditions can be improved in order to make more conclusive results, finalizing the low pressure printing chamber being one of the improvements. Exploring potential mixture modifications and performing improved tests using the basis laid in this report might lead to a potentially effective and realistic way of utilizing Martian regolith for unmanned 3D-printing purposes with minimal investment, which is one of necessary goals in making a manned Martian mission possible.

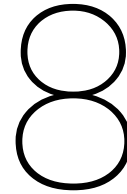
First of all, the curing of the mixture in suboptimal conditions, namely pressures of 0.1 and 0.01 bar, and temperature below 23°C, makes the resultant mechanical properties significantly worse as compared to higher pressure and temperature. From the results of moulding tests, the robustness of the samples cured at decreased pressure and temperature conditions as compared to room conditions is not sufficient for building purposes at all, as large amount of the samples are too weak to withstand the preload (0.5 N) of the three-point bending test. The decrease in pressure makes water present in the mixture to rapidly evaporate, halting the polymerization reaction as water presence is necessary for oligomer mobility. Also, it leaves empty space in the material bulk as the result of bubbles formed through water boiling. These boiling induced pores are visible upon the material inspection (0.1-0.4 mm at 0.1 bar cure, 0.4 mm and higher at 0.01 bar cure), unlike the small pores

that are formed as water pockets during 1 bar pressure cure. Combined with the low reaction rate due to low temperature, this leaves the material bulk mostly unreacted. Low amount of polymeric links makes the material very weak, decreasing flexural strength and elastic modulus.

Secondly, the printability of the mixture with the available 3D-printer is unsatisfactory. Viscosity of the mixture is highly dependant upon the regolith to binder ratio. Low viscosity, such as at 65% regolith concentration or lower, makes the mixture easily extrudable, but upon deposition the shape is not kept as the mixture flows over the build plate. On the other hand, high viscosity, such as at 68% regolith concentration or higher, requires a relatively large printing syringe outlet diameter (over 7 mm) and high pressure (over 1 bar) to be pushed out in the first place. Under extruding pressure, even as small as 0.3 bar relative pressure, the mixture inside the syringe cures rapidly, making it too solid to be further printed. The samples that managed to get printed had overall lower mechanical properties than samples moulded at the same curing conditions, as average ultimate flexural strength dropped by 20%. The flow of the mixture induced inhomogeneity in reaction progression along the material bulk, hence preventing polymeric links from forming between some areas. This is another argument for using as high outlet as possible.

Another issue with the current binder composition is the necessity to use a large amount of it with respect to regolith. Minimal binder to regolith ratio that was achievable during the testing phase was 30%, which is a large amount to be brought from Earth. The limitation in this case was wetting the regolith powder enough so all of it is incorporated in the mixture. Considering that overall mechanical properties of the mixture increased with the increased regolith content, a change in the binder composition to incorporate more regolith per binder amount should also be made. With a considerable technological advancement, it might be possible to extract and synthesise binder components directly on Mars, as all required elements (hydrogen, oxygen, either sodium or potassium) are present there. Such solution however is very futuristic at the moment.

The results of testing the samples cured at room conditions and better, in particular at higher temperature, were very satisfactory with good robustness and high average flexural strength of 2.5 MPa and higher. This particular mixture has a chance to be a viable space building material solution with enhanced composition (optimised binder solution with incorporated hydroxide, optimal regolith ratio) and artificial increase in temperature and pressure curing conditions. However, a considerably higher amount of work is yet to be done to come close to the perfect solution.



## Recommendations

Large number of variables that had to be evaluated with respect to mixture properties (regolith ratio, binder composition, cure pressure and temperature) resulted in a limited amount of samples that could be produced for each situation due to time constraints. Because of this, evaluations of elastic modulus and flexural stress dependencies were limited to the mentioned properties only, and some important observations were potentially missed. Some curing conditions did not produce samples robust enough to go through the testing process, which also caused inconclusive results like in Figures 6.11 f) and g), and hence outlines the boundaries for curing conditions of the proposed mixture. Simply conducting more tests for each curing condition up to the boundary ones would give more data and help improve the analysis. Potential analysis improvements also include more conclusive data on the optimal binder concentrations and regolith fractions in the mixture, as missing points and outliers obtained in this report skewed that data considerably.

**Narrowing down mixture compositions.** Although the mixture properties were acceptable when cured at high temperatures, the performance when cures at low pressures and temperatures was unsatisfactory. Not only mechanical properties were considerably lower, but also overall robustness was unacceptable. It is known that adding a strong base into the mixture increases alkalinity of the binder, providing the reaction with an easy source of  $OH^-$  particles. In room temperature/pressure and above, mechanical properties of such enhanced geopolymer are known to be better, and quantifying how much better these properties are would help to further optimize the mixture. Introducing such extra variable into the scope of this report was not possible because of time constraints and safety concerns. Using the results of mechanical testing performed in this report, it is possible to eliminate certain mixture compositions as they are inferior, which can reduce the amount of further testing with more variables.

**Enhancing the mixture by adding hydroxide.** One significant variable that was eliminated from the general picture is the use of a hydroxide in conjunction with Sodium Silicate in a binder compo-

sition. By increasing alkalinity of the mixture, all reaction steps occur at a higher rate, forming larger amount of polymeric bonds in a shorter period of time. Potentially, this can offset the negative effect of low pressure on mechanical properties, as the reaction can happen to a further extent before water is gone from the mixture. Same goes for negative effect of temperature, as the cure can happen faster at higher alkalinity. Most importantly, it might reduce the required amount of binder, as powder dissolves in alkaline medium at a higher rate. It is however expected that the optimal balance between silicon and aluminum might shift due to the preferred formation of  $[SiO_2(OH)_2]^{2-}$ , which is suboptimal when it comes to geopolymerisation. Hence, the addition of hydroxide into mixture in varying quantities can be tested together with the effect of it on the mechanical properties.

**Printer design adjustments.** Due to time constraints and initial concept of 3D-printer vacuum chamber not working out, printing in conditions different from room ones was not performed. However, considering poor results from curing the moulded samples at low pressures and temperatures, printed samples are expected to perform as poorly in these conditions as in the case with room condition cure, if not worse. Before printing experiments can be continued, the mixture composition has to be improved considerably. From the mechanical property observation it is implied that increasing the syringe outlet diameter improves the result through lower pressure requirement for deposition and better material homogeneity. Hence, it would make sense to attempt changing the printer design to allow large outlet diameter. Such change can also increase the viscosity margin, allowing more viscous paste to be printed, which in real application would reduce the amount of binder to be brought from Earth.

**Extensive post-production evaluation.** While this report is concerned with the curing conditions of the proposed binder/regolith mixture, it is also important to look at the performance of this material in extreme conditions after being cured. Materials like Portland cement exhibit poor mechanical properties when it comes to ambient temperature swings. Thorough mechanical testing of improved mixture is required in order to proceed with printing adjustments, including compression test in addition to flexural or tensile stress test, and thermal fatigue test among the most important ones.

**Exploring other binder options (polymers).** Overall, in current form the mixture looks hardly suitable for 3D-printing on Mars, and a large amount of adjustments are needed to make it work. From the other binder options, the option of using polymer was hardly explored by the literature, but can potentially be a really good solution if investigated properly. Engineering a polymer that can incorporate regolith powder well and cure in Martian ambience with minimal investment is surely a very challenging task, but can potentially be done. In the end, for planning an actual Mars mission, it is best to explore as many options and propositions as possible in order to select the one with the least risk and price involved.



# Bibliography

- [1] P. Duxson et al. Geopolymer technology: the current state of the art. *Journal of Materials Science*, 42(9):2917–2933, dec 2006.
- [2] J. Davidovits et al. Geopolymers: man-made rock geosynthesis and the resulting development of very early high strength cement. *Journal of Materials education*, 16:91–91, 1994.
- [3] Techcon Systems. Tsr2000 series 3 axis dispensing robot - hardware instruction manual. *Version 1.2*, 2018.
- [4] Techcon Systems. Tsr2000 series 3 axis dispensing robot - teaching pendant user guide. *Version 1.2*, 2018.
- [5] Ulbrich group webshop. Techcon systems ts350 digital fluid dispenser. <https://www.ulbrich-group.com/techcon-systems-ts350-digital-fluid-dispenser>, retrieved 15/08/2019, 2019.
- [6] Conrad Electronic Benelux webshop. Tru components tec1-12706 peltier-element. <https://www.conrad.nl/p/tru-components-tec1-12706-peltier-element-15-v-64-a-65-w-l-x-b-x-h-40-x-40-x-38-mm-189115>, retrieved 09/08/2019, 2019.
- [7] The Martian Garden webshop. Mms-2 enhanced mars simulant. <https://www.themartiangarden.com/mms2/mms2>, retrieved 18-08-2018, 2019.
- [8] S. Raval. Exploration colonization resource extraction and utilization of moon and mars. *Astronautical Congress IAC, Cape Town (South Africa) volume 9 p.p. 7845-51*, 2011.
- [9] NASA. Apollo 11 mission overview. [https://www.nasa.gov/mission\\_pages/apollo/missions/apollo11.html](https://www.nasa.gov/mission_pages/apollo/missions/apollo11.html), retrieved 08 – 2018, 2019.
- [10] F. Slakey et al. Robots vs. humans: Who should explore space? *Scientific American sp*, 18(1):26–33, feb 2008.
- [11] L. Bettiol et al. Manned mars mission risks evaluation. *69th International Astronautical Congress (IAC), Bremen, Germany*, 2018.
- [12] F. A. Cucinotta et al. Space radiation risk limits and earth-moon-mars environmental models. *Space Weather*, 8(12):n/a–n/a, dec 2010.
- [13] G. Horneck et al. HUMEX, a study on the survivability and adaptation of humans to long-duration exploratory missions, part II: Missions to mars. *Advances in Space Research*, 38(4):752–759, jan 2006.

- [14] V. Bhim et al. Opportunities and constraints of closed man-made ecological systems on the moon. *Advanced space research volume 14 p.p. 271-280*, 1994.
- [15] B. Kading et al. Utilizing in-situ resources and 3d printing structures for a manned mars mission. *Acta Astronautica*, 107:317–326, feb 2015.
- [16] Megan Gannon. 3d printer could transform moon dirt into lunar base. <https://www.space.com/18694-moon-dirt-3d-printing-lunar-base.html>, retrieved 13-06-2018, 2012.
- [17] F. Ceccanti et al. 3d printing technology for a moon outpost exploiting lunar soil. In *61st International Astronautical Congress, Prague, CZ, IAC-10-D3*, volume 3, pages 1–9, 2010.
- [18] M. Bodiford et al. In-situ resource-based lunar and martian habitat structures development at NASA/MSFC. In *1st Space Exploration Conference: Continuing the Voyage of Discovery*. American Institute of Aeronautics and Astronautics, jan 2005.
- [19] Silvia Benvenuti, Fabio Ceccanti, and Xavier De Kestelier. Living on the moon: topological optimization of a 3d-printed lunar shelter. *Nexus Network Journal*, 15(2):285–302, 2013.
- [20] Kanako Hayatsu, Makoto Hareyama, Shingo Kobayashi, Naoyuki Yamashita, Mitsuhiro Miyajim, Kunitomo Sakurai, and Nobuyuki Hasebe. Radiation doses for human exposed to galactic cosmic rays and their secondary products on the lunar surface. *Biological Sciences in Space*, 22(2):59–66, 2008.
- [21] Youngmin JeongAhn and Renu Malhotra. The current impact flux on mars and its seasonal variation. *Icarus*, 262:140–153, 2015.
- [22] PA Bland, TB Smith, AJ Timothy Jull, FJ Berry, AWR Bevan, S Cloudt, and CT Pillinger. The flux of meteorites to the earth over the last 50 000 years. *Monthly Notices of the Royal Astronomical Society*, 283(2):551–565, 1996.
- [23] H. Toutanji et al. Strength and durability performance of waterless lunar concrete. In *43rd AIAA Aerospace Sciences Meeting and Exhibit*. American Institute of Aeronautics and Astronautics, jan 2005.
- [24] T. D. Lin et al. Concrete lunar base investigation. *Journal of Aerospace Engineering*, 2(1):10–19, jan 1989.
- [25] C. Montes et al. Evaluation of lunar regolith geopolymer binder as a radioactive shielding material for space exploration applications. *Advances in Space Research*, 56(6):1212–1221, sep 2015.
- [26] M.H.Y. Kim et al. Radiation protection using martian surface materials in human exploration of mars. *Physica Medica*, 17:81–83, 2001.

- [27] Jun Liu et al. Effect of low temperature on hydration performance of the complex binder of silica fume-portland cement. *Journal of Wuhan University of Technology-Mater. Sci. Ed.*, 29(1):75–81, feb 2014.
- [28] E. Obonyo et al. Advancing the use of secondary inputs in geopolymer binders for sustainable cementitious composites: A review. *Sustainability*, 3(2):410–423, feb 2011.
- [29] B. Singh et al. Geopolymer concrete: A review of some recent developments. *Construction and Building Materials*, 85:78–90, jun 2015.
- [30] S. Sen et al. Multifunctional martian habitat composite material synthesized from in-situ resources. *Advances in Space Research*, 46(5):582–592, sep 2010.
- [31] Y. JeongAhn et al. The current impact flux on mars and its seasonal variation. *Icarus*, 262:140–153, dec 2015.
- [32] H. Y. McSween et al. Elemental composition of the martian crust. *Science*, 324(5928):736–739, may 2009.
- [33] M. Mikoc et al. Alkali-activated fly ash concrete (concrete without cement). *Technical Gazette*, 18(1):99–102, 2011.
- [34] F. Puertas et al. Alkali-activated slag concrete: Fresh and hardened behaviour. *Cement and Concrete Composites*, 85:22–31, jan 2018.
- [35] F.G. Collins et al. Workability and mechanical properties of alkali activated slag concrete. *Cement and concrete research*, 29(3):455–458, 1999.
- [36] L. Weng et al. Dissolution processes, hydrolysis and condensation reactions during geopolymer synthesis: Part i—low si/al ratio systems. *Journal of Materials Science*, 42(9):2997–3006, jan 2007.
- [37] T. Bakharev et al. Effect of elevated temperature curing on properties of alkali-activated slag concrete. *Cement and Concrete Research*, 29(10):1619–1625, oct 1999.
- [38] Test method for short-beam strength of polymer matrix composite materials and their laminates.
- [39] B. M. Jakosky et al. The mars atmosphere and volatile evolution (MAVEN) mission. *Space Science Reviews*, 195(1-4):3–48, apr 2015.
- [40] NASA. Mars fact sheet. 2016, retrieved 01-06-2018.
- [41] M. Nesarajah et al. Thermoelectric power generation: Peltier element versus thermoelectric generator. In *IECON 2016 - 42nd Annual Conference of the IEEE Industrial Electronics Society*. IEEE, oct 2016.